NTNU

Norwegian University of
Science and Technology

Oil/ Paper Insulation for HVDC: Conductivity of Oil

Emmanuel Akuffo Nartey

Master of Science in Electric Power Engineering
Submission date: June 2011
Supervisor: Frank Mauseth, ELKRAFT

Norwegian University of Science and Technology
Department of Electric Power Engineering

PROBLEM DESCRIPTION

The electric field distribution in a HVDC converter transformer is determined by the relative resistivity of insulation components (oil, paper, and pressboard). However, there is today no specific procedure for measuring oil conductivity for oils for HVDC converter transformers. It is disputed whether oil conductivity and functionality is reduced with time when in-service. Measuring techniques are disputed, reflected by the fact that IEC operates with two different techniques (IEC 61620 and 60247). Moreover, there is insufficient knowledge to specify under which conditions such tests should be performed for converter applications. Transformer oil has a strong non-linear conductivity, depending on geometry and stress history. It is influenced by chemical composition, temperature, moisture and electric field, and it has been shown that the conductivity and field distribution changes with time under operating conditions in a composite insulation system. This may potentially lead to dielectric stresses during transformer tests being lower than in service. If new special requirements for HVDC transformer-oils are to be introduced it is important that these reflect the functional needs for uses in converter transformer.

During the master thesis the student should:

- Describe theory/model for conductivity
- Perform measurements with and without an oil-flow
- Investigate the oil conductivity as a function of voltage, frequency and temperature

The measurements should be done on both new and used/aged transformer oil

Supervisor: Frank Mauseth

ACKNOWLEDGEMENT

My sincere thanks go out to my supervisor Frank Mauseth for taking time to supervise my work.

A big thanks you to Stian Ingebrigtsen for dedicating so much of his limited time to aid me and guide me throughout the period of the work. I really appreciate all your efforts

I am appreciative of the all the help I had from Dag Linhjell of Sintef Energy during the setting up and conduct of the experiments; without your help I would not have gone far.

To all the other people at Sintef energy: Lars Lundgaard and Espen Eberg for their contributions and counsel.

Last but not the least, to my family; I say a big thank you for their support.

ABSTRACT

The work begins with a theoretical description of conductivity and the importance of this material property in the electrical power industry. The various theories describing high voltage conduction in highly insulating dielectric liquids are analysed to ascertain their propensity to explain the exponential rise in the conductivity of the insulating liquid at high fields.

The work goes further to analyse the various methods and standards that are presently utilised in the measurement of conductivity of highly insulating oils. The short-comings of the present methods particularly the IEC 61620 and 60247 are identified. The physics behind the peculiar behaviour of the conductivity when stressed under high electric fields is described and analysed.

Measurements carries out according to a standard, may not lead to useful results. Therefore, it is preferable to determine the conductivity under practical aspects and also to measure the different parameters on which the conductivity depends (1). A new method of carrying out conductivity measurements based on the use of triangular and sinusoidal input high voltage is used in this work.

Conductivity analysis is carried out based on this method while time dependency, frequency dependency and field dependencies are studied.

The results of the various results show a strong dependency of the resistance of the oil on the input electric field up to two powers of ten; when the electric field is varied from zero to 10 kV/mm for all frequencies. The frequency of input voltage has a minimum effect of the results of the conductivity up to 0.1 Hz; the only observable change is the increasing values of the capacitive current component of the measured total current.

The time dependency of the resistance values shows a very remarkable variation of conductivity. There is an average of 3 times in the conductivity when the oil is stressed over a 24 hour period.

Finally Comsol Multiphysics simulation is carried out to compare to the results of the experimental results obtained in the laboratory. The results of the current as well as the resistance values obtained using the comsol simulation bears great similarity to that of the laboratory experiments.

Table of Contents

List of Figures

CHAPTER 1: INTRODUCTION

Electrical insulating systems have traditionally been utilised in the isolation of electronically live parts from other live parts or ground. They vary in form and shape: solid, liquid or gaseous. They are characterised by their ability to contain stresses emanating from high electrical fields. This characteristic is known as the dielectric strength.

All dielectrics are designed to isolate the electrically live parts from other live parts or from the ground. They must therefore be able to withstand the electric fields for which they are designed without breaking down. In addition to insulating live parts of equipment, the insulation system also endures physical and chemical stresses as a result of their interaction with the outside environment. The insulation system must be able to function appropriately in spite of the conditions for the lifetime of the equipment. As such, insulation systems are about the most import parameter to consider when designing a power system.

An under specification or a defect in the insulting systems to be utilised in an equipment could result in total damage with consequences of fatalities. In order to avoid such mishaps with catastrophic effects, it is imperative to have standard parameters by which to measure and grade the suitability of a particular insulation system for a specific task. One such important parameter of much interest is the dielectric strength of the material. It is the voltage per unit material thickness that can be applied to the dielectric before it breaks down. The higher the dielectric strength of the material, the higher the electric stress it can endure and the more suitable it is to be used for higher voltage systems.

Liquid dielectrics which in almost all cases are combined with solid insulating systems are most preferred because they among others offer a very efficient thermal dissipation, a high density and as such a high dielectric strength, ability to be metamorphosed into several geometries and their ability to self heal or recover their dielectric capabilities after an electric arc as with gas-insulating systems (2)(3). The liquid dielectrics are characterised by their dielectric strength, permittivity and electrical conductivities. These characteristics influence their choice of use in particular systems. Liquid dielectrics have a wide range of usage in modern power systems as they serve as insulating systems in transformers, cables, switchgears among others.

The conductivity of the insulating liquids which is the focus of this project is a parameter which is describes the ability of the insulating liquid to conduct current when a voltage is

applied across it. It is as a result of the ionisation of the atoms of the oil. When a voltage is applied across the insulating oil, the atoms get ionised and move within the liquid the movement of the charge particles within the liquid carries the current. The greater the number of charge particles which are usually electrons, the greater the conductivity and the higher the current that can be conducted. The conductivity of a dielectric liquid is a measure of the charge carrier concentration at thermal equilibrium.

The electric conductivity of dielectric liquids is one of the most important parameter characterising the electric properties of these materials. It gives information on the insulating state of the material and on its behaviour in the presence of an electric field. It also gives information on the purity, essentially ionic, of the liquid. In electrical engineering, in particular for transformers, cables and capacitors, both pieces of information are of great interest for the choice of the liquids, the quality checks for manufacturing and, in some cases, for monitoring during service (4)

Most insulation systems utilising liquid dielectrics are utilised in conjunction with solid dielectrics forming what is known as two-phase dielectrics. In transformers, they are used together with paper and pressboard. They fill in cavities within the paper to minimise partial discharges in addition to insulating the windings and conducting heat. In such multi-phase insulating systems, the electric field is divided between the different dielectrics based on either their permittivity or conductivities. On the application of an alternating voltage across the insulating system, the electric field distribution among the dielectrics is based on their permittivity while on the application of a direct current (DC) voltage across the insulating system the field is distributed based on the conductivities of the dielectrics(5).

High Voltage Direct Current (HVDC) transmission offers many advantages to the power system. It offers among others the possibility to transmit large magnitudes of power over long distances which would be otherwise very inefficient if Alternating Current (AC) transmission were used. It also affords the possibility to interconnect systems operating on different frequencies.

High Voltage Direct Current (HVDC) transmission offers many advantages to the power system. It offers among others the possibility to transmit large magnitudes of power over long distances which would be otherwise very inefficient if Alternating Current (AC) transmission

were used. It also affords the possibility to interconnect systems operating on different frequencies.

These merits of the HVDC systems come with the requirements of building specialised equipment to handle the peculiar challenges of HVDC. These include the construction of converter transformers. Converter transformers are specially designed to handle the normal stresses of ordinary power transformers as well as additional DC stresses resulting from the HVDC. The stresses in the insulation demands that the transformer insulation systems (both the pressboard and the oil) should be dimensioned to handle these stresses.

Modern power systems the world over are expanding at an unprecedented pace as a result of the increase in population and the increasing standard of living of the populace. This expansion puts much stress on the power system as such a remedy has been the utilisation of high voltage direct current transmission systems(HVDC) which boasts a higher power transfer capability per surface area of conductor utilised. This type power transmission method requires big infrastructure in terms of converter stations and converter transformers. Converter stations impute a direct voltage component in addition to the normal alternating current voltage component. As a result, the stress on the converter transformers is a combination of the grid alternating voltage with a superimposition of the direct current voltage from the converter switches

The conductivity of the highly insulating dielectric oils are anomalous in nature in that, it does not fall in well with the established laws of electrolytic conduction as observed in liquids of higher conductivity (6). This anomalous conductivity of highly insulating dielectric oils is described and investigated in this work.

The electric field distribution in a normal power transformer is distributed between the oil and paper in relation to their permittivities but in the case of converter transformers the direct current supposed of the alternating current leads to a distribution of the electric field

- The electric field distribution in a HVDC converter transformer is determined by the relative resistivity of insulation components (oil, paper, and pressboard) solemn
- Transformer oil has a strong non-linear conductivity, depending on geometry and stress history (electrical and thermal)

The general state of knowledge in the conduction and breakdown of dielectric liquids is not as advanced as that of solid and gaseous dielectrics. Though many aspects of the dielectric liquids has been investigated by many researchers over the years, the findings and conclusions from the different researchers cannot be reconciled to produce a general theory applicable to insulating liquids due to the variation and sometimes contradictory nature of the results. The principal reason for this could be attributed to the lack of comprehensive theory on the physics of the liquid state which would form the foundation by which observations could be compared and related (7).

There is the difficulty of investigating the behaviour of individual components in a composite material as such to fully characterise the insulation system, individual components must be initially characterised.

In order to determine the required minimum time to stress the oil to obtain steady state conductivity values, the oil sample would be stressed for a very long time the current values test cell is analysed to ascertain the instance that steady current values are obtained.

Since the required solution of the thesis work should be the ability to replicate real conductivity values as in real life situations in HVDC transformers, the values obtained must be steady state values under high electric stresses as pertained in real HVDC transformers. The IEC 61620 and 60247 standards on oil conductivity are lacking in this regard since they only focus on initial conductivity values.

Most standards on conductivity values make use of direct current (DC) stresses in the measurements but this work focuses on the use of alternate signals in the measurements. This would be compared to the results obtained in when direct current (DC) stress is used.

High Voltage Direct Current (HVDC) Converter transformers in real life are stressed by power frequency (AC) superimposed on a Direct Current (DC) electric stress of high magnitudes.

These high stresses act on the total insulation system which is paper/pressboard and transformer oil. Such high stresses experienced by the insulation system for the entire lifecycle of the transformers require that they are designed and built to withstand them. In addition to the design stage, condition monitoring of the insulation system are needed to reduce cost, to be able to keep old transformers for as long as possible , to improve the

reliability of the power system by reducing the failure rate, to improve insulation coordination among others by revealing trend analysis.

The insulation system must be tested with electric stresses similar to that in practice to able to correctly dimension the insulation to meet such operational stresses.

The conductivity of the oil is a strong indication of the purity and quality of the insulation. The measurement of the conductivity of the conductivity of the oil is therefore pivotal to the determination of the quality and as such the condition of the whole insulation system. The importance of the determination of exact values cannot be overemphasised.

Though various researchers have different views as to the physics of the conduction process at elevated electric fields, the results of the experiments are somewhat similar as they point to a particular direction. From the literature, it can be inferred that the under high electric field stress, the conductivity of the insulating oils have an initial period of decreasing conductivity with increasing field strength. The conductivity reaches a minimum at approximately 3kVpermm after which there the conductivity rapidly increases with field strength (8)(9). The Figure 1-1 shows the graph of resistivity against electric field.

The resistivity measurements of oil impregnated cellulose materials show better reproducibility than that of free oils. The oils have a rather stochastic behaviour due to differing modes of the sweeping of ions within the oil and as such carrying out repetitive experiments show wide disparities even when carried out under similar conditions.

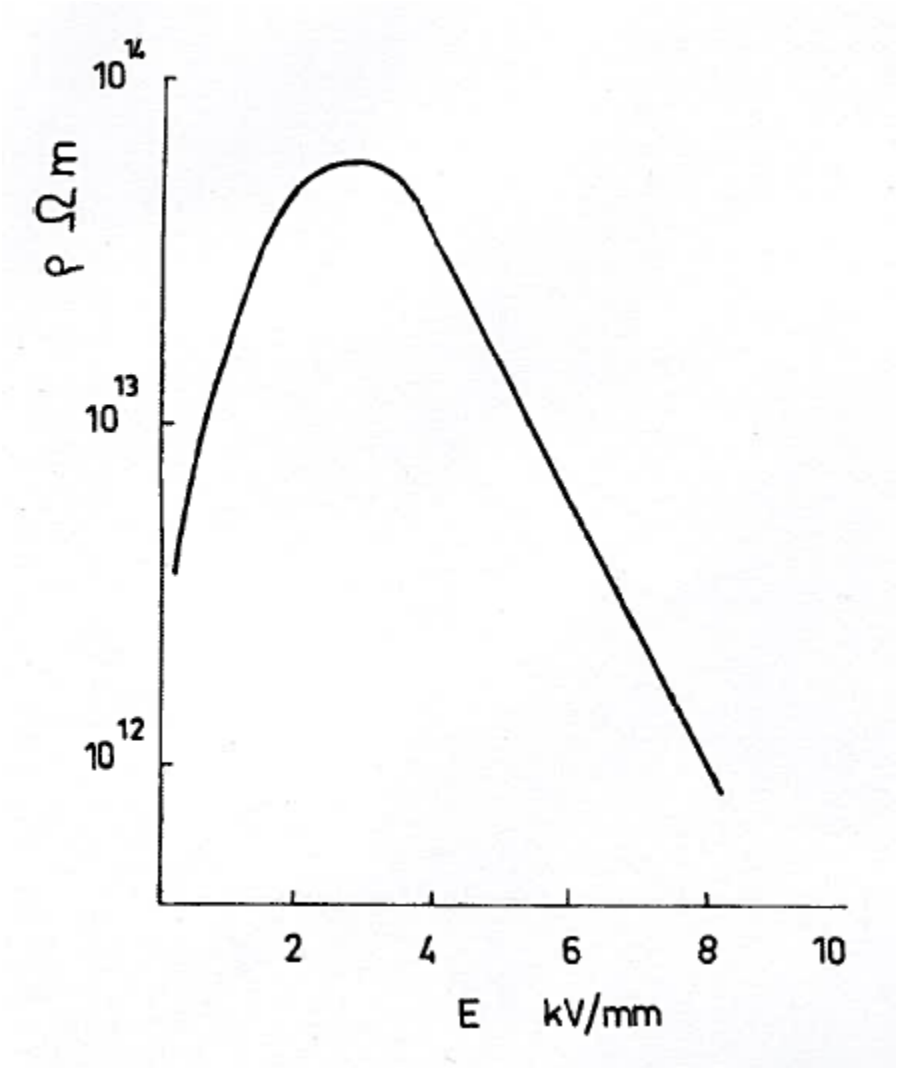

Figure 1-1 Oil resistivity as a function of the Electric field strength for new dry oil (9)

CHAPTER 2: THEORY OF CONDUCTION

The conductivity of a dielectric liquid is a measure of the charge carrier concentration at thermal equilibrium (10). Conduction in liquids is unlike the conduction in solids as the electrons are cannot flow freely; as such for the liquid to conduct there must be the present of ionised or dissociated products.

Measuring the conductivity of a liquid is not straight forward. And as such presents an experimental problem (11). According to Ohm's law, conduction current density *j*, when an electric field *E* is applied is given by

$$j = \sigma E \qquad [2.1]$$

Where j is the current density

σ is the conductivity

E is the electric field

The conductivity is the result of free carriers in the bulk of the liquid or injected into it by the electrode. If there are i different carrier species within the liquid each with a mobility μ, charge density q and n is the number density of each species, the conductivity would be given by

$$\sigma = \sum_i \mu_i q_i n_i \qquad [2.2]$$

2.1 High Field Conduction Mechanisms

Conductivity at elevated field stresses deviate from the values obtained under low field stresses. The currents are substantially increased as the electric field is increased. The conductance of the insulating oils deviate considerably from Ohm's law as such the law has a limited range of validity when high electric fields are considered.

Various researchers have propounded several theories intending to explain the physics behind conduction at elevated electric fields. The varying views on the physics of high field conduction in non linear media as oil could be traced to the fact that different researchers obtained different results. The non-unifying explanations given by various researchers would be examined (12).

The influence of the electric field on the conduction could be categorised into two distinct mechanisms: bulk mechanism and interfacial mechanism.

Bulk mechanism are concerned with interactions that occur within the bulk of the oil sample away from with no interaction with the electrode surface whiles the interfacial mechanisms refer to mechanisms that occur at the interface between the metal electrode and the bulk oil sample. In the literature, a number of both bulk and interfacial mechanisms have been postulated to explain the apparent increase in the conductivity of dielectric oils at elevated electric fields.

Bulk mechanisms include collision ionization and avalanche formation, field-enhanced ionic mobility and field enhanced dissociation of electrolytes while the interfacial mechanisms described in the literature include electron emission from cathodes and oxidation or reduction of neutral species at the electrode surface.

2.1.1 Collision ionisation and avalanche formation

With regards to collision ionization and avalanche formation, electrons gather enough energy from the electric field to ionize neutral atoms through inelastic collisions thereby increasing the number of ions and electrons available to conduct the electrons. The magnitude of the increase in conducting species within the bulk of the liquid is proportionate to the increase in the conductivity of the sample. Although this is possible, it could only occur at extremely high fields up to several MV/cm (13). Collision ionisation is therefore not to be expected in a liquid for electric fields less than the intrinsic breakdown strength of most organic solids (14).

2.1.2 Field-enhanced ion mobility

The theory of field enhanced ion mobility which was postulated by G I Skanavi(14) is brought about from two main explanations, firstly, the new mobilities of the ions when stressed under electric field jump from one location to the other with the separation(δ) between adjacent sites comparable to molecular diameter , that is a few 10^{-8} cm. Usually, the drift velocity in a material is directly proportional to the electric field, which means that the electron mobility is a constant ($v = \mu E$), where v is the velocity, μ is the mobility and E is the electric field. When the electric field is increased above a threshold, the mobility of the ions depends on the electric field.

$$v \propto \sinh(E\delta / 2U) \qquad [2.3]$$

where v is the mean velocity, $U = kT/e$. If $E\delta/2U \leq 1$, the ion mobility is proportional to the electric field *(E)* but when the value of $E\delta/2U \geq 1$, the law is exponential. Since this effect cannot occur at relatively low voltages this effect can be ignored (13).

A more practical explanation would be the electrohydrodynamic (EHD) convection. This phenomenon occurs at relatively lower electric fields (approximately at 10 kV). With this phenomenon, ions are carried about together with the liquid flow. Since the liquid flow is considerably faster than the ion drift, the ion transport is enhanced by a factor reported in the literature to be $\sqrt{M}$, where M is the ratio between the electrohydrodynamic mobility ($\sqrt{\frac{\varepsilon}{\rho}}$) where ρ is the specific mass of the oil and the true mobility of the ions (15). The enhanced mobility does not create any additional charge carriers within the bulk oil; it only increases the drift velocity.

2.1.3 Field-Enhanced Dissociation

Lars Onsager's work on deviation from Ohmic laws for weak electrolytes explains the dependence of the electric conductivity on the applied electric field. The weak electrolyte is assumed to contain a certain concentration of neutral particles and another concentration in equal amounts o positive and negative ions. The dissociation rate of neutral ions to form positive and negative ions is controlled by the dissociation constant *(K_D)* while the rate at which free ion pairs recombine to form neutral ion is controlled by the recombination constant *(K_R).*

$$AB \underset{K_R}{\overset{K_D}{\rightleftarrows}} A^+ + B^- \qquad [2.4]$$

According to Onsager, the dissociation constant K_D, is dependent on the electric field while the recombination constant is invariant with the field. The field dependency of the dissociation constant would result in the increase of the ion pairs at elevated electric fields culminating in the increase in the conductivity of the weak electrolyte.

$$K_D = K_D^0 \cdot F(E) \qquad [2.5]$$

Where :

$$F(E) = I_1(4b)/2b \qquad [2.6]$$

With I_1 been a modified Bessel function of the first order and

$$b = \left(q^3 E / 16\pi\varepsilon_0\varepsilon_r k^2 T^2\right)^{1/2} \quad [2.7]$$

k is Boltzmann's constant, T is the temperature and E is the electric field.

While:

$$K_R = q\left(\mu_p + \mu_n\right) / \varepsilon_0\varepsilon_r \quad [2.8]$$

Where

The potential well binding the positive and negative ions to an ion pair is distorted by an applied electric field and will be lowered with increasing field. A lowering of the potential barrier will increase the dissociation rate of the ion pair (16).

The theory stems from Lars Onsager's theory work on deviations from Ohm's law in weak electrolytes (17). In this theory, Lars states that when an ion pair is in the electric field, the positive ion is escapes in the direction of the field. The potential barrier opposing separation is lowered with respect to the zero-field condition by an amount equal to ΔV whose calculation is identical to that of the Schottky effect. With

$$\Delta V = \sqrt{eE / \pi\varepsilon} \quad [2.9]$$

The probability of the separation will be enhanced by the factor $F = e^Z$, where

$$Z = \sqrt{\left(eE / \pi\varepsilon\right)} / U \quad [2.10]$$

The enhanced separation of the ions is only valid when the electric field is in the direction is the positive direction. The observed current rise due to the field enhanced dissociation of ions with voltage can be accounted for only when the dielectric constant of the liquid is low such as in hydrocarbons. The rise of current with increasing voltage can however be the result of electrode injection at the interface between the electrode and the bulk liquid dielectric.

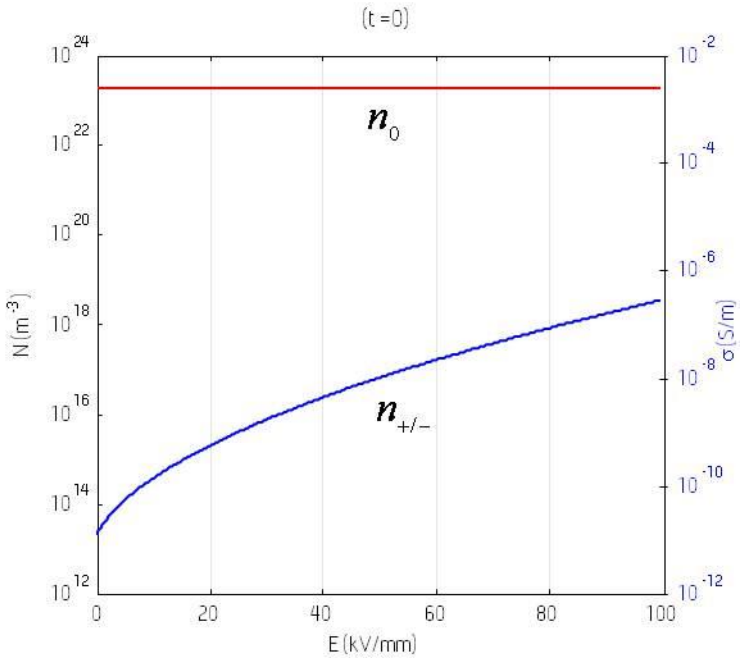

Figure 2-1 Increased concentration of ions with increasing electric field due to field enhanced dissociation

The Figure 2-1 shows the exponential rise in the number of ions with an increase in the electric field as a result of field-enhanced dissociation. These additional ions increases the

The technique of distinguishing between either of the two modes is the response of the current with time when a step voltage is applied. While the current first increases with time before increasing due to the wave of charge-carriers in electrode injection, the current during decreases monotonously when bulk dissociation is the mechanism at work.

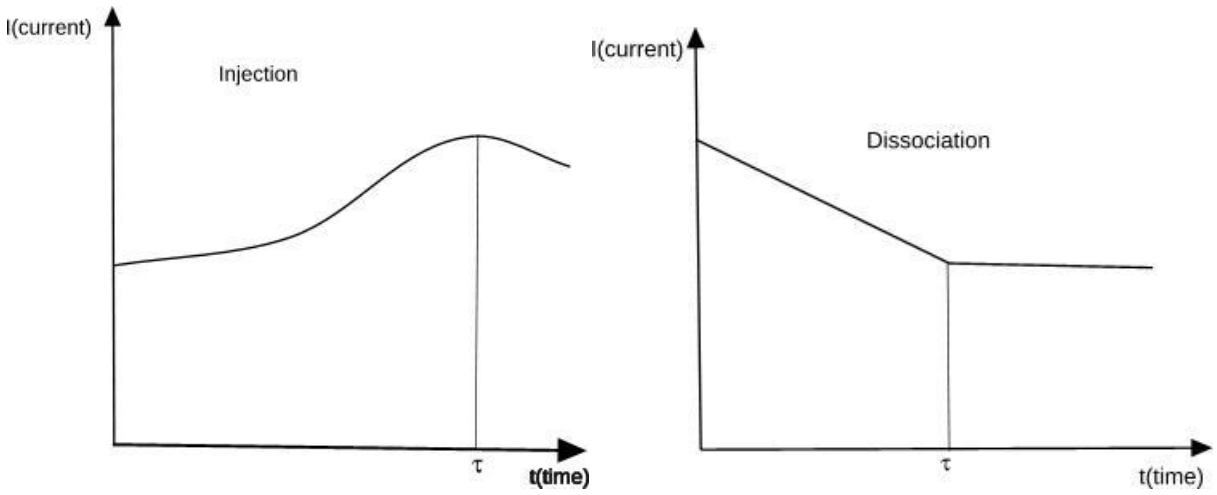

Figure 2-2 Graph showing current-time plots under step voltage. The graph to the left shows the variation when there is electron injection and that to the right when there is bulk dissociation. τ is the flight time of the electron

The most popular interface mechanism at high electric field is the electrode injection. The interface between the bulk oil and the electrode surface is clearly the initiation point of the electron injection into the bulk of the oil.

2.1.4 Field Emission

The possibility of electron transfer between adjacent phases is well documented (13). This mechanism is well understood in vacuum where it is described by the Fowler-Nordheim formula,

$$J = \left(AE^2/W\right)e^{\left(-BCW^{1.5}/E\right)} \qquad [2.11]$$

Where $A = e^3/8\pi h$, W is the work function, E is the electric field, $B = 8\pi\left(2m\right)^{0.5}/3heE$, C is a function of $y = e^{1.5}E^{0.5}/\left(4\pi\varepsilon_0\right)^{0.5}W$ which represents the Schottky lowering of the Work force (W-barrier). It decreases monotonously form 1 to 0 when E increases from 0 to 1.

From the above equations, it can be inferred that there is a strong dependency of the current density *(J)* on the Electric field *(E)*. Though carrier injection or quantum-mechanical tunnelling of electrons from electrode is highly probable, the use of the Fowler-Nordheim equation on field emission and Schottky's thermionic emission equation without any adjustments leads to erroneous conclusion since there were derived for electron emission from a clean electrode to vacuum. Experimental current-voltage characteristic of the oil must be used to modify them (18).

The electric field as such would provide the electrons at the surface of the electrode with energy to overcome the barrier. The level of electric field required is ≈ 10^6V/cm. However, surface protrusions on the electrode are likely to lead to concentration of the electron injection in one or more filamentary paths. This leads to the theory of filamentary single injection postulated by Kwan C. Kao (12).

The filamentary single injection theory is based on the following postulate:

The high field conduction is mainly due to electron emission from the unavoidable asperities on the metallic cathode surface and is confined to one or more filamentary paths, in which the current density is much larger than that in other regions (12). The electric conduction becomes filamentary because the electrode surface is not microscopically identical in asperity and surface conditions from domain to domain. Thus there may be one or more micro-regions in

which the potential barrier has a profile more favourable for carrier injection than in other regions. Furthermore, the bulk oil under high field strength is not microscopically homogenous when electrohydrodynamic motion sets in (19). As a result of these uniformities, the electric field between two plane electrodes is not uniform longitudinally due to space charge injection and the current density is also not uniform as a result of filamentary current flow. The proponent of the filamentary current injection give a further support of this theory by citing the fact that the electric breakdown channel is always filamentary no matter the medium; liquid, solid or gas and the fact that the surface of an electrode has only a tiny spot of damage in the event of an electric breakdown (12).

According to Onsager, the initial separation of the ions before the application of the electric field is applied is not of immense importance as the magnitude of the field. In his opinion, the effect of the electric field is to increase the fraction of the escaping ions by a factor which in the incipient stage is proportional to the field intensity. In numerical terms the predicted increase in the ionisation current is about 1% for every 100V/cm.

The applied field strength lead to undesired effects, field accelerated dissociation which raises the conductivity at electric fields (E) higher than 1 kV/cm. Above this field strength, charge injection plays a significant role, which depends on the liquid used, impurities and the electrode material. Also because ion current flow goes together with material transport, especially for high viscous oil types, electro-hydrodynamic fluid movements can cause an additional charge transport. This leads to an apparent increase in the conductivity above field strength of 100 V/cm.

2.1.5 Electrochemical Conduction

Electrochemical conduction may be the result of either electrolytic dissociation of the solutes or (rarely) of the liquid itself or carrier injection at liquid/electrode boundary. It is a ubiquitous phenomenon and could be wither an oxidation or reduction of neutral species at the liquid/metal interface. This phenomenon generates both negative and positive charge carriers. There is electron transfer between the metal and the adsorbed neutral species; the electron has to tunnel through a barrier at the electrode/oil interface. Electronation is a fast process and as such would not determine the overall rate of electrochemical conduction. After the electronation, the resulting ion overcomes a barrier due to thermal excitation. When a strong enough electric field is applied, the barrier is lowered with a corresponding steep

increase in the current. The current density *J (E)*) is therefore depends on the barrier at the interface (13).

2.2 Status today

The currently available method for the determination of the conductivity of highly insulating liquids, for which transformer oil is inclusive are carried out in accordance with the international electrotechnical commission (IEC) 60247 and 61620 standards.

2.2.1 The IEC 61620

The IEC 61620 standard describes a method for simultaneously measuring of the conductance and capacitance enabling the calculation of the dissipation factor of insulating liquids. The method covers both unused insulating oils and insulating oils in service in transformers and in other electrical equipment.

The standard works on the principle of measuring both the capacitive and conductive currents by applying an alternate square wave voltage to the test cell. The capacitive current is measured during the rise time and the conduction current is measured during the stable period of the voltage.

The measurement technique utilised a square voltage of amplitude between 10 and 100 V, frequency between 0.1 Hz and rise time between 1 msec and 100 msec. The standard recommends carrying out the experiment at ambient temperature but gives room for carrying it out at other temperatures.

2.2.2 The IEC 60247

The standard describes a method for describing the determination of the dielectric dissipation factor (tan δ), relative permittivity and dc resistivity of insulating liquid material at the test temperature. The test is applicable to both unused and service oils. According to the standard, a dc electric stress of 250 V/mm is applied for a period of (60 ± 2) s after which the current and voltage are recorded. The resistivity of the oil is calculated as the using the formula below:

$$\rho = K\frac{U}{I} \qquad [2.12]$$

where

U is the reading of the test voltage in volts

I is the reading of the current in amperes

K is the cell constant in metres.

The cell constant calculated from the capacitance according to

$$K(m) = 0.113 \times capacit\,an\,ce(pF) \qquad [2.13]$$

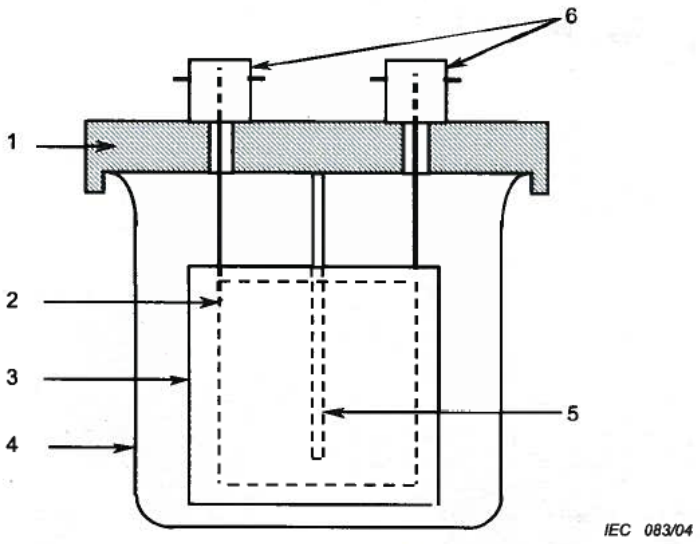

Key

1	cover
2	inner electrode
3	outer electrode
4	stainless steel vessel
5	sheath for temperature measurement
6	BNC plugs for electrical connection

Figure 2-3 Test cell design for the IEC 61620 and IEC 60247 (20)(21)

2.2.3 Temperature Dependence of the Conductivity

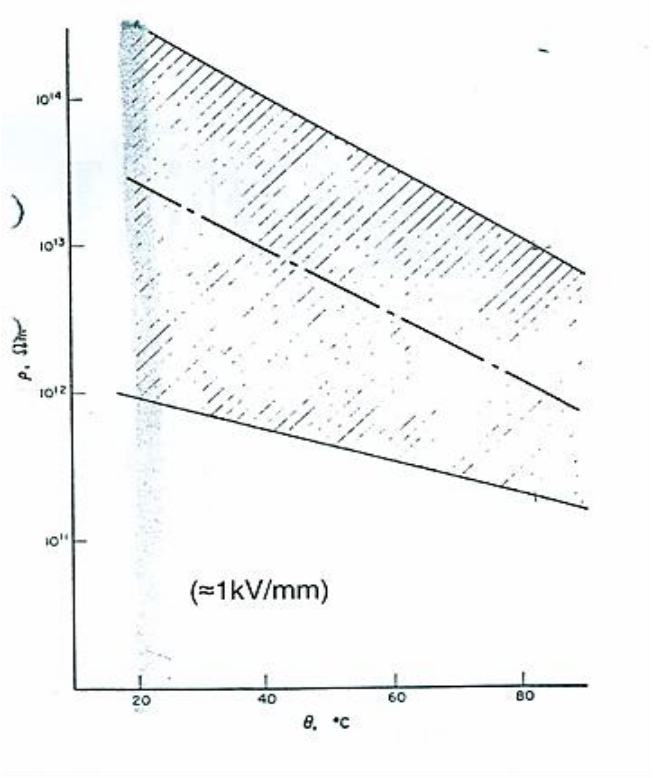

Figure 2-4 Graph showing the temperature dependence of the conductivity of un-aged oil

From the literature, there is the observance of about a decade increase in the conductivity of the oils when the temperature of the oil is increased from 20°C to 60°C

2.2.4 Stages In The Conductivity With Increase In the Electric Field

Theoretical treatment and various experiments conducted by various researchers have pointed to a particular trend in the conductivity values measured with increasing electric field. The literatures suggest three main stages in the development of the conductivity values with increasing electric field.

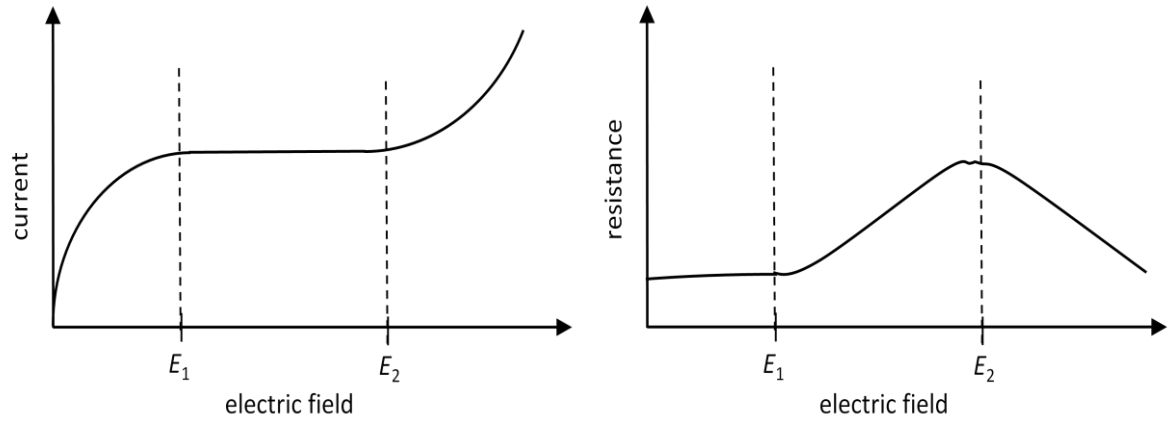

Figure 2-5 Graph showing the change in the current with increasing field (left) and the variation of the resistance with increase in field (right) (14)

In the first stage ($E< E_1$) which follows Ohmic laws, the free ions available for conduction are consumed as soon as they are produced within the bulk oil: as a result, the conductivity remains at a constant value.

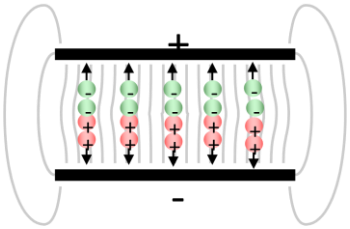

Figure 2-6 Diagram showing the production of ions instantaneously as they are produced

In the next stage ($E_2>E>E_1$), there is a decline in the conductivity value with an increase in the applied electric field. At this stage, there is a net decrease in the number of ions available for conduction since the ions are swept away from the gap at a faster rate than they are produced

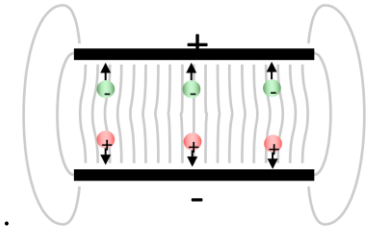

Figure 2-7 A depiction of the sweeping away of ions from the bulk of the oil than they are produced

In the final stage ($E>E_2$), the effect of the high field comes in to force as more ions are produced by varying means more than they are swept out of the gap.

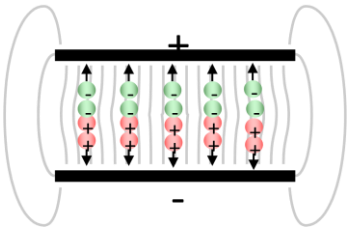

Figure 2-8 Production of more ions than are swept away

2.3 Limitation of Current Standard

It can be inferred for the above two standards that, the time period during which the oil ample is stressed is limited with the IEC 61620 recommending an immediate recording of the current and voltage reading while the IEC 60247 recommending the reading of the data after a minute of stress. Real life transformers are stressed for time periods exceeding the times recommended by the standards, more over many electrodynamic activities take some time to reach equilibrium. When an insulating liquid is under electric stress, the current is highest in the initial stage and gradually decays to a stationary value after a period of time. As a result, any conductivity measurement solely based on initial current values does not reflect the dc stationary conductivity of the liquid.

It is clear that the stress level recommended for both standards are far below the electric stress experienced by the insulation system under normal field conditions as such. While the IEC 61620 requires the use of a voltage of use a voltage of 10 V, the IEC 60247 recommends a voltage level of which falls short of the normal expected field stresses which are in the range of a few kilo Volts per mm. As such methods would not give a fair judgement as to the conductivity value of the oil. This is because the conductivity of insulating oils is not as constant as the permittivity which varies very little but on the contrary can vary in the range of two powers of ten over a wide electric field range.

The standardised methods of conductivity measurements have adopted the use of low voltage methods in order to eliminate effects such as charge carrier injection or electrode polarisation which may result from the use of high voltages (22).

CHAPTER 3: SET-UP AND METHODOLOGY

In this experiment, high voltage triangular waves are applied to a plane-to-plane electrode arrangement, and the current through the oil is measured at the lower electrode.

The input signal is supplied from a signal generator. The signal generator can be manually regulated to produce specific amplitudes and frequencies of varying wave types. The experiment starts with the choice of a triangular wave shape with increasing amplitudes to 10V peak. A choice of low frequencies from 0.01 to 1 Hz is used in the experiments.

The input wave form from the signal generator is connected to the input terminal o the Trek™ high voltage amplifier the high voltage amplifier has a constant amplification of 2000V/V with a maximum current delivery of 20mA. The Trek high voltage amplifier is mounted on a sturdy rack and separately connected to the mains via an isolated power receptacle. The connection between the signal generator and the high voltage amplifier is made with a coaxial cable.

A low noise current amplifier is connected to the output of the test cell, which amplifiers the current signal before it is connected to the oscilloscope. The sensitivity (magnification) of the current amplifier is manually adjusted to give a high enough current capable of been read by the oscilloscope and at the same time low enough to fall within the prescribed limits of the current amplifier. The sensitivity is thus not kept constant but varied in proportion to the current from the test cell.

The oscilloscope receives signals from three different sources which are connected to three different channels from the four available channels of the oscilloscope. The signal generator is connected the first channel , signal monitoring output of the high voltage amplifier is connected to the second channel while the output of the current amplifier is connected to the third channel of the oscilloscope through a custom-made low pass filter.

Customised LabView software is made which controls and automates data reading from the three channels of the oscilloscope. The software communicates with the oscilloscopes through the USB port via a National Instruments USB controller by which it triggers and receives data from the various ports of the oscilloscope. The program effectively sends trigger signals to the oscilloscope after a manually set time delay which corresponds to the time required to get a whole screen shot from the oscilloscope. After a full screen of the various signals is obtained, the programme holds the signal for the electrical data to be saved on the computer in ASCII-

text format. The programme stores each measurement as a unique file with a file name which is specified by the user. The user manually sets the time duration between readings of the measurements. The picture below shows the front panel as well as the detailed Virtual Instruments used in the programme (VI).

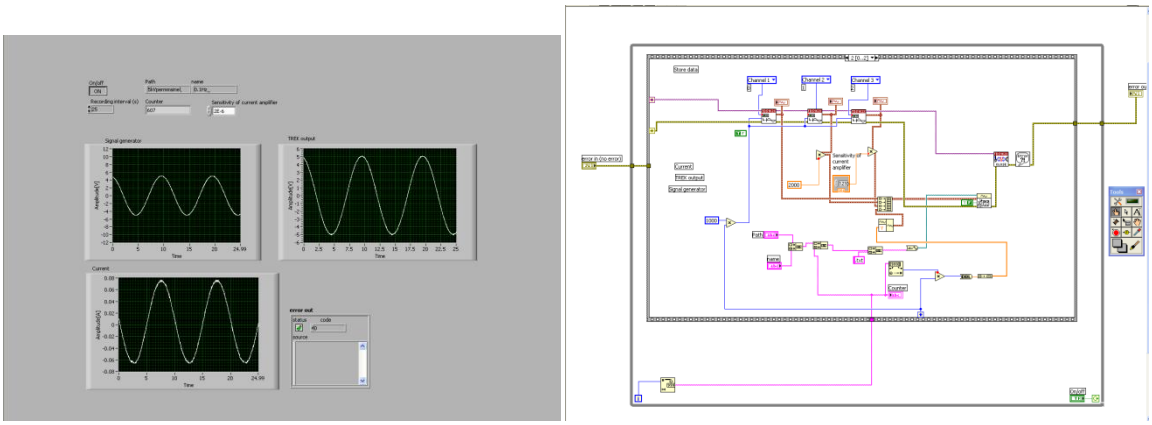

Figure 3-1 Screenshot of the front panel (shown on the left) and part of the Virtual Instrument (VI) (on the right side of the screen) written in labview to control and automate the reading of data from the oscilloscope

3.1 The Oil

The oil used is the Nynas Nytro 10XN, which is super grade oil manufactured form naphthenic oil. It has low viscosity at high temperatures and excellent solvency. It also has high oxidation stability. The oil is a clear and bright inhibited super grade that conforms to both ASTM D3487 and the IEC 60296:03 including the fulfilment of specific requirements. It has outstanding oxidation stability as well as a maximum resistance to oil degradation. It is specifically designed for use in oil-filled electrical equipment including transformers, rectifiers, circuit breakers and switchgears. The oil is manufactured by the Nynas company according to the IEC 60296/03 standard.

The transformer oil, in this case, Nynas Nytro 10XN is placed in a closed glass vessel also containing the electrodes. In addition to these properties, the Nytro 10Xn has a high dielectric strength. Enough oil is poured to completely submerge the electrodes in order to mitigate possible partial discharges. The test cell is then sealed and placed on a rack in the forced draught oven. Coaxial cable is connected to the lower electrode which conducts the current from the oil to the low noise current amplifier. The high voltage probe is also connected to the upper electrode through a low pass filter which attenuates the noise superimposed on the signal before it is connected to the test cell.

Since high voltages are used in the experiments, a safety and security feature is inculcated in the initial design of the experimental setup. A micro-switch is attached to the door of the forced-draught oven which disconnects the high voltage supply when the door of the oven is accidental opened. This prevents inadvertent contact with the high voltage supply.

3.2 The Test Cell

The test cell is made of borosilicate glass sealed on both ends with a wooden board with a rubber O-rings to avoid the leakage of the oil. The electrodes are made of brass, each with an area of 63.617 cm^2 and thickness of 1.1 cm. The lower electrode is fixed while the upper electrode is attached to a retractable armature permitting the variation of the gap distance. The retractable armature has a cavity at its apex which serves as a receptacle for attaching the high voltage probe. The lower electrode has a guard ring attached to it its lower face which is connected to ground potential to avert edge effects during measurements.

The test cell can be cleaned by unscrewing the bolts that hold the glass containment to the wooden boards at both ends. The electrodes can then be individual removed to make way for thorough cleaning. The test cell is filled with oil by unscrewing the bolts that hold the upper wooden board to the glass cell.

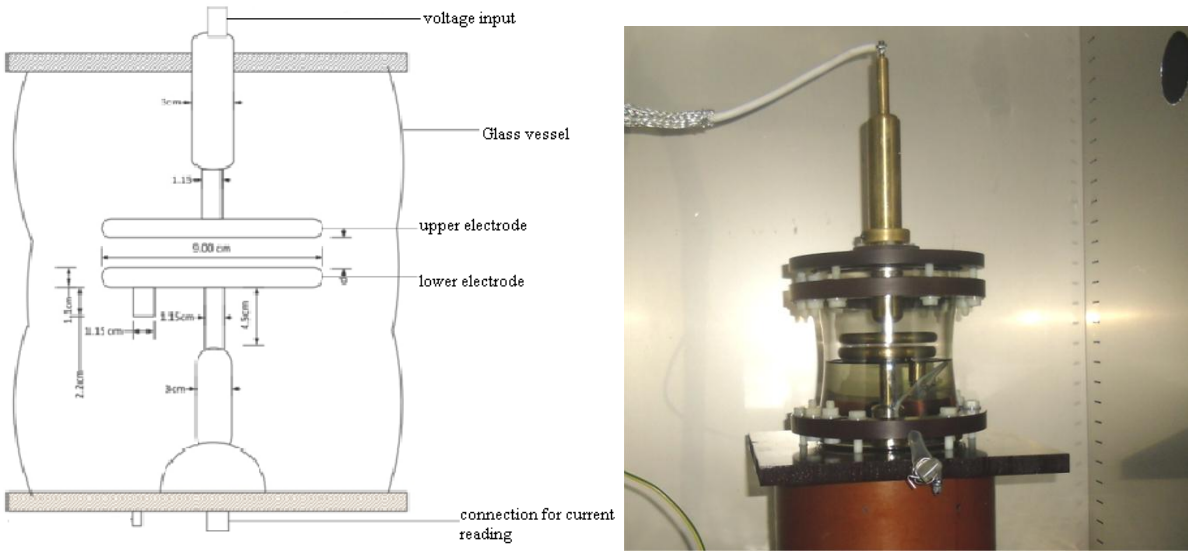

Figure 3-2 diagram (left) and picture (right) of the cylindrical test cell with plane-to-plane electrode geometry

Two different methods are used in the experiments; the first method makes use of a triangular wave generated from the signal generator which is connected to the high voltage amplifier. The high voltage signal is then connected to the test cell through the low pass filter while the second method makes use of a sine wave instead of a triangular wave.

Both methods are measured at varying frequencies; 0.01, 0.1 and 1 Hz. The current, voltage signal and the high voltage input values for each experiment are automatically registered by the customised LabView™ programme. The programme automatically saves the data as text files which are later exported into Matlab for data processing.

Each experiment is carried out for a long enough period to approach steady state conditions. On average about two hundred readings are taken for each experiment to ensure a good average results.

Before the measurements are taken, the test cell is properly cleaned and allowed to dry overnight to totally rid it of moisture, also, enough time is allowed for the oil to stabilise and to remove all gas bubbles which would otherwise interfere in the measurements of correct current values or on the more serious side cause a breakdown.

The results of the various experiments are saved as text files. The files are then imported into Matlab where the analysis is done. The Matlab programme reads the numeric data from the text files while ignoring other files which are not needed by the programme.

The matlab programme first opens a dialogue box, where the user selects a desired number of files to analyze. The number of files selected is dependent on the number of files that would be averaged in the programme. The selected files are copied into the matlab programme.

The data read into the matlab programme include the current, input signal and high voltage values at each sampling interval, the time between the readings of the oscilloscope data, the sampling interval.

These data are read into memory and used by the matlab programme where the calculation of the various parameters takes place. The programme calculates the capacitive current and subtracts it from the total current recorded. The remaining current, the resistive current is used in the calculation of the conductivity of the oil sample.

Parameters of special interest in the analysis of the data from the experiments include but not limited to the resistance and current. The variation of the current with time is also investigated to gain knowledge on the dependence of the resistance with time.

In processing in the data, a number of assumptions were made that were implemented in the matlab programme. The total current is the sum of the conducting and capacitive currents. The capacitive current is calculated and subtracted from the total current to obtain the conducting current.

3.3 The triangular wave method

This method which has been developed and used by the ABB with good results in the lower voltage levels is used at elevated electric fields in this work. In the low voltage method, the signal generator generates a triangular wave of frequency 0.01Hz and amplitude of 10V while the current amplifier amplifiers the output signal from the test cell before the signal is connected to the oscilloscope. The sensitivity of the amplification used depends on the magnitude of the current from the test cell. The test cell is made of stainless steel cylindrical electrodes of thickness 1 mm. The test cell has a volume of 200 cm^3 for the large cell and 15 cm^3 for the smaller cell. It has a stainless steel sheath for dipping a temperature probe for the measurement of the temperature of the containing liquid. The Figure 3-4 shows the setup for the measurement of the conductivity of insulating oils using the triangular wave method.

The low field conductivity of the insulating oil which is related to the charge carrier concentration at thermal equilibrium is determined by applying the low frequency (0.01 Hz) triangular wave of low voltage (10 V) to the stainless steel test cell. After recording the current as a function of time (see Figure 3-5), the magnitudes of the displacement and resistive currents can be easily separated from the shape of the current- time curve. The conductivity is then calculated as the ratio of the resistive to the capacitive current, knowing the permittivity of the oil and the period of the voltage wave (22).

$$\sigma = 4 \cdot \frac{\varepsilon_r \varepsilon_0}{\tau} \cdot \frac{I_R}{I_C} \qquad [3.1]$$

Where $I_{R\ and}\ I_C$ are respectively the resistive and capacitive currents

τ is the period of the voltage wave

ε_R and ε_0 are the relative permittivity and permittivity of free space respectively.

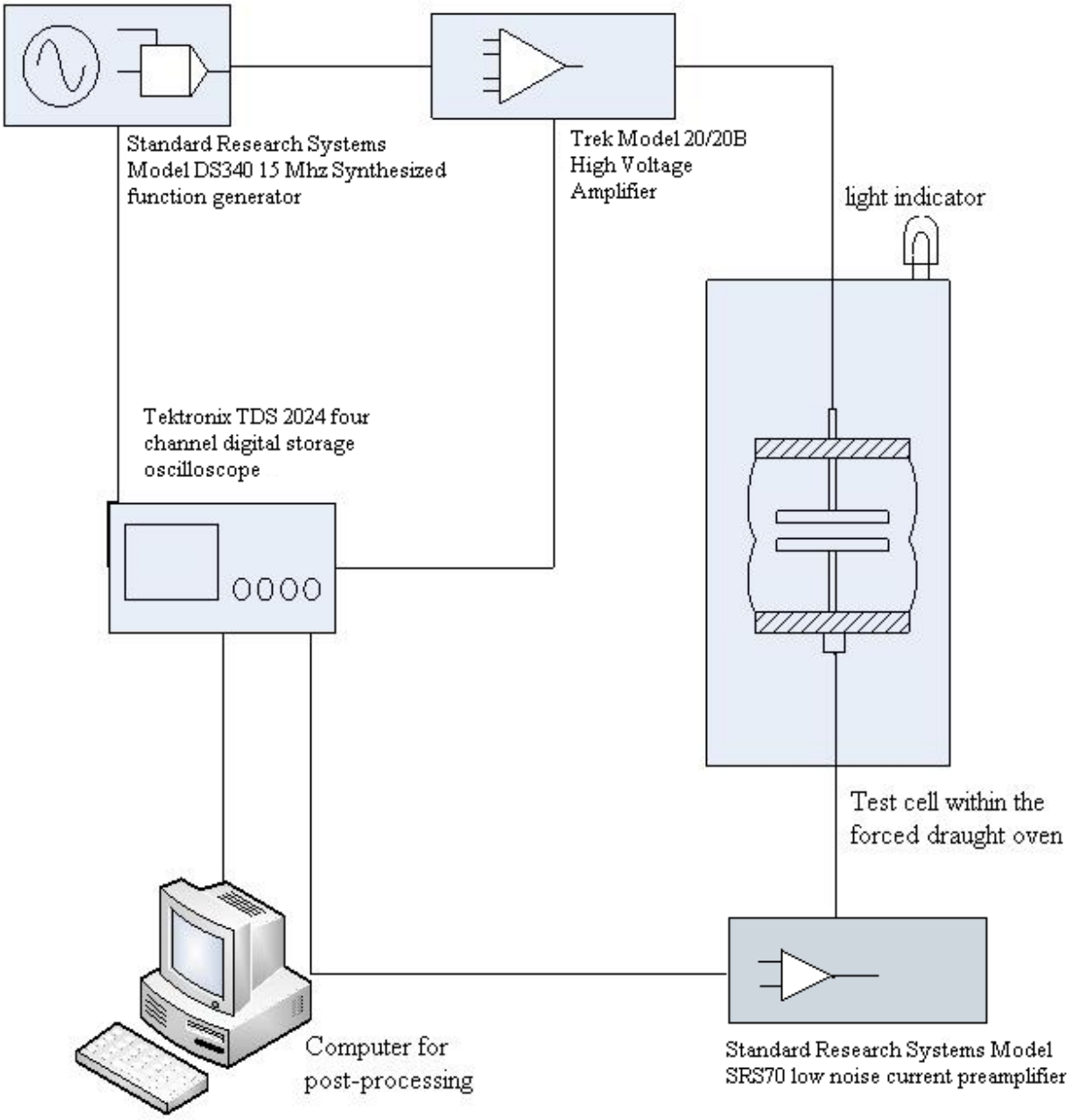

Figure 3-3 Laboratory Setup for the measurement of conductivity of insulating oils using high electric fields

Coaxial cables connect the signal generator, the current amplifier and the Trek High voltage amplifier to the oscilloscope. A specialised power cable connects the output of the Trek high voltage amplifier to the test cell while the oscilloscope is connected to the Computer through a USB-USB isolator by a USB cable. In the bid to avoid the coupling of noise signals unto the current readings, the power cable linking the Trek high Voltage amplifier to the test cell as well as the coaxial cable linking the test cell to the current amplifier are shielded.

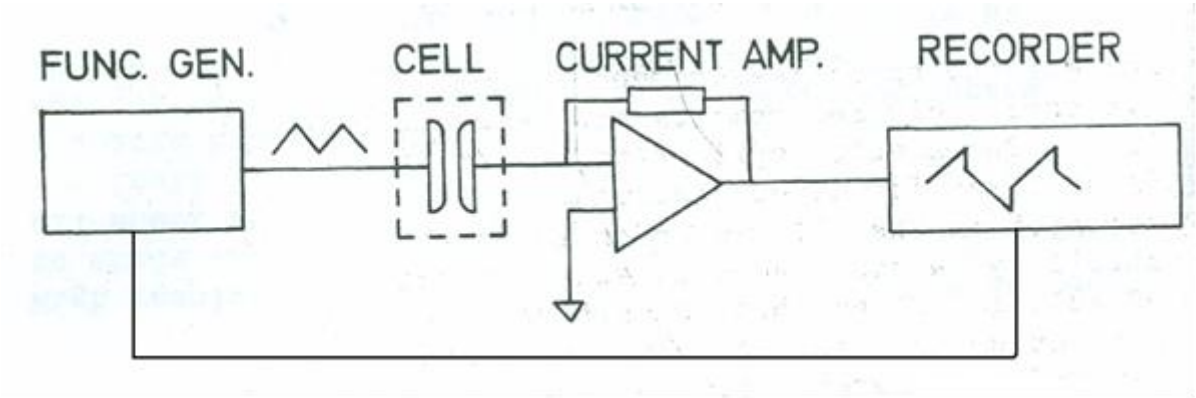

Figure 3-4 Schematic diagram of the setup used in the low field triangular wave (ABB) Method of conductivity measurement (23)

The conductivity of the oil is calculated from the values of the conducting current and capacitive current derived from the current waveform.

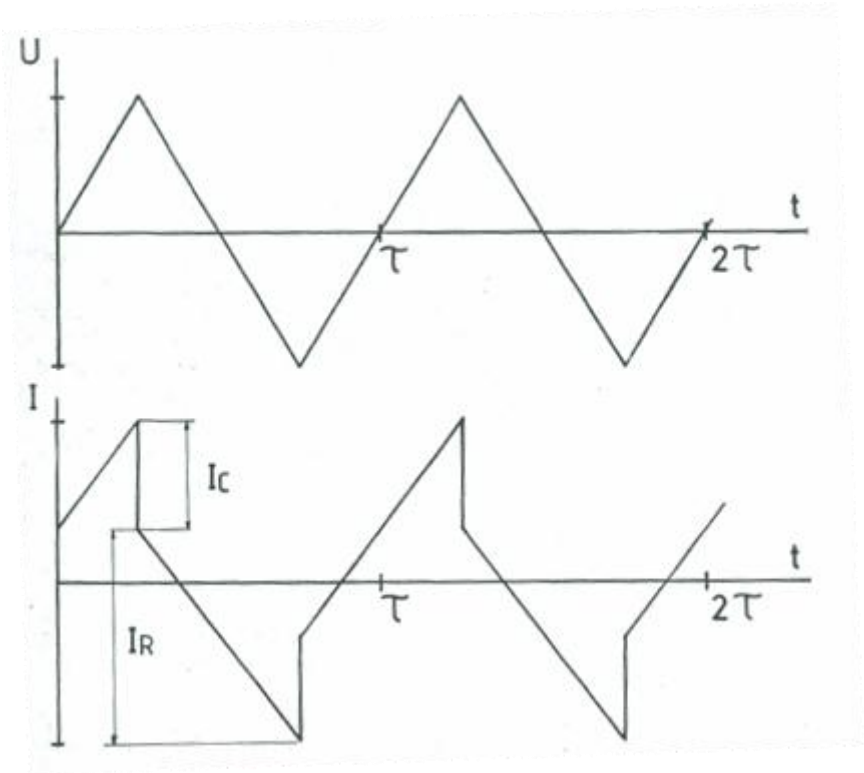

Figure 3-5 Graph of input triangular wave (upper figure) and the expected current output (lower curve). Where τ is the period of the wave, I_c is the capacitive current and I_R is the resistive (conductive) current (23)

Since the triangular wave method works quite well at low voltages, it is serves as the first option to use when the study of conductivity of highly insulating dielectric liquids is to be

studied at elevated electric fields. The signal to be used is easily obtained from standard signal generators and is amplified using the Trek™ high voltage amplifier.

The high voltage signal is connected to the upper electrode of the test cell via a cable which is doubly shielded as a safety precaution. The male jack lead of the cable is fixed into the cavity in the retractable armature connected to the upper electrode through a low pass filter.

Measurements are carried out at various electric fields from a minimum of 1 kV/mm to a maximum of 10 kV/mm. The constraint to upper limit of the electric field is the limitation of the Trek™ high voltage amplifier. The amplifier has a maximum output of 20 kV.

3.4 The Sine Wave Method

The sine wave method which employs a sinusoidal waveform of varying frequencies is used in this experiment. This method is serves as an alternate method of carrying out the experiment.

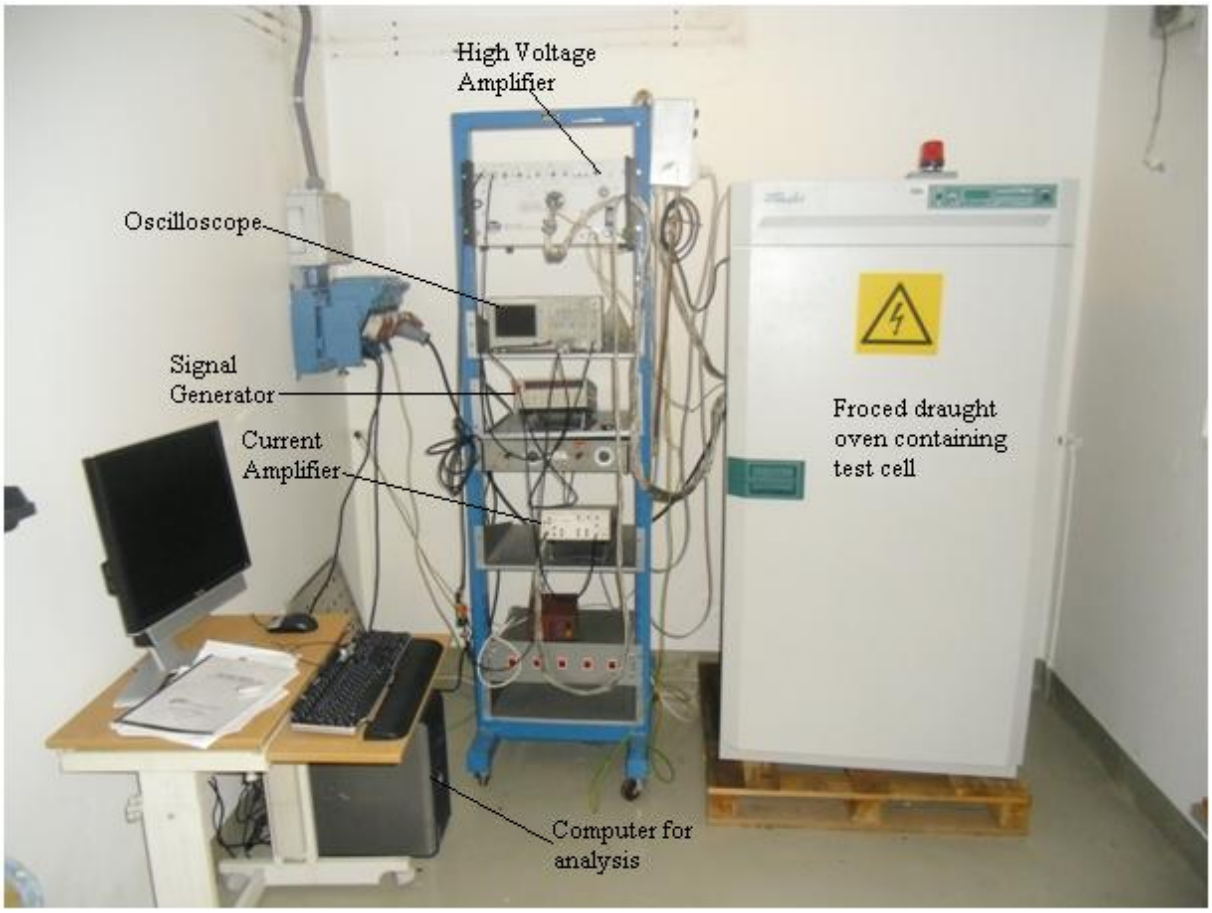

Figure 3-6 The Set-up for the laboratory work. The test cell is housed in the forced draught oven. Oscilloscope communicates with the computer.

The sine wave method also uses the same set-up as the triangular wave method shown in the Figure 3-3. The only parameter that is changed is the shape of the signal.

CHAPTER 4: RESULTS

The results of each experiment are displayed as curves showing the currents (conductive and total), the input high voltage and finally the resistance. Another programme extracts the time dependency of the resistance values.

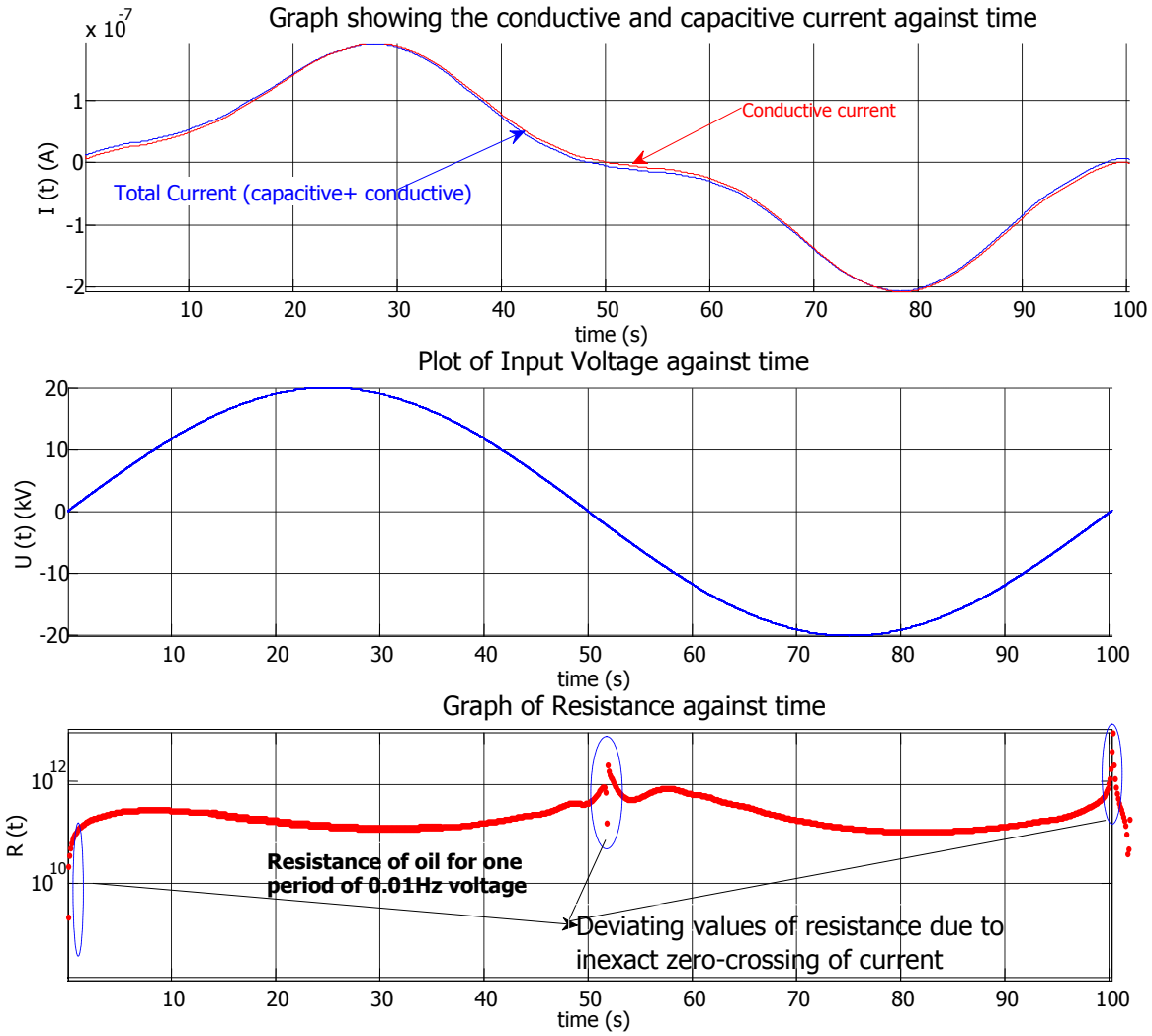

Figure 4-1 Plots showing the currents (total current and calculated conductive current), input high voltage and calculated resistance against time for frequency of 0.01 Hz

4.1 Field Dependence of the Resistance

In this section of the results, analyses of the effect of the field on the resistance values of the oil at varying electric fields are carried out. In the analyses, the results of both the triangular wave and the sinusoidal wave methods are presented. The results of the triangular wave

method are presented with peak electric field strength of 10kV/mm while the sinusoidal wave method is presented for both 5 and 10 kV/mm.

The results show the trend of the resistance of the oil for both the positive half and negative half of the electric field; as such the development of the resistance during the rising half as well as the falling half of the electric field is visualised. The results concentrate on three frequencies: 0.01 Hz, 0.1 Hz and 1 Hz.

4.1.1 Triangular Wave Method

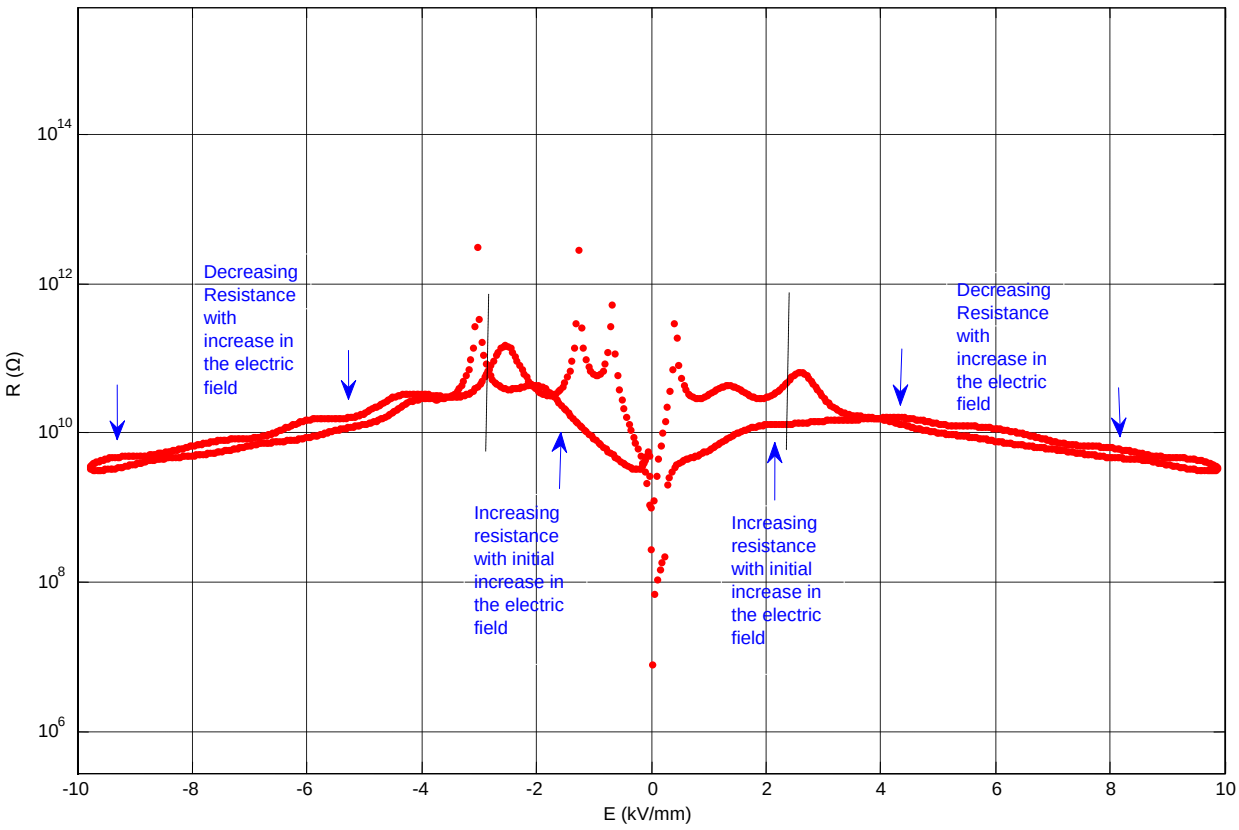

Figure 4-2 Graph Showing the variation of the resistance with increase in the Electric Field for a frequency of 1 Hz

In the Figure 4-2, the resistance values of the oil when stressed with by 10 kV/mm, 1 Hz triangular electric field is shown. The resistance value fall within two powers of ten. It can be seen that the resistance increases almost linearly with increase in electric field for both polarities up to 2.348 kV/mm for the positive polarity and 2.77 kV/mm for the negative polarity where maximum resistance is attained. After this threshold field, there is a monotonic decrease in the resistance for the rest of the range of electric field used in the experiments.

The results show a decrease from the maximum of $1.104 \cdot 10^{-11}$ A which occurs at the field strength of -2.77 kV/mm to a minimum of $3.532 \cdot 10^{-9}$ A at -10 kV/mm representing almost two decades reduction for a 7.072 kV/mm increase in the electric field.

One other observation from the graph is that the resistance obtained during the rising half of the wave deviates slightly from that during the falling half of the wave for both the positive and negative polarity voltages. The resistance values close to zero electric field had erroneous values due to the numerical deviation of the current values at the zero crossing of the input high voltage signal.

4.1.2 Sine Wave Method

After the oil sample is stressed for under a high electric field of 10 kV/mm, the effect of the stress on the conductivity value is analysed and plotted in Matlab.

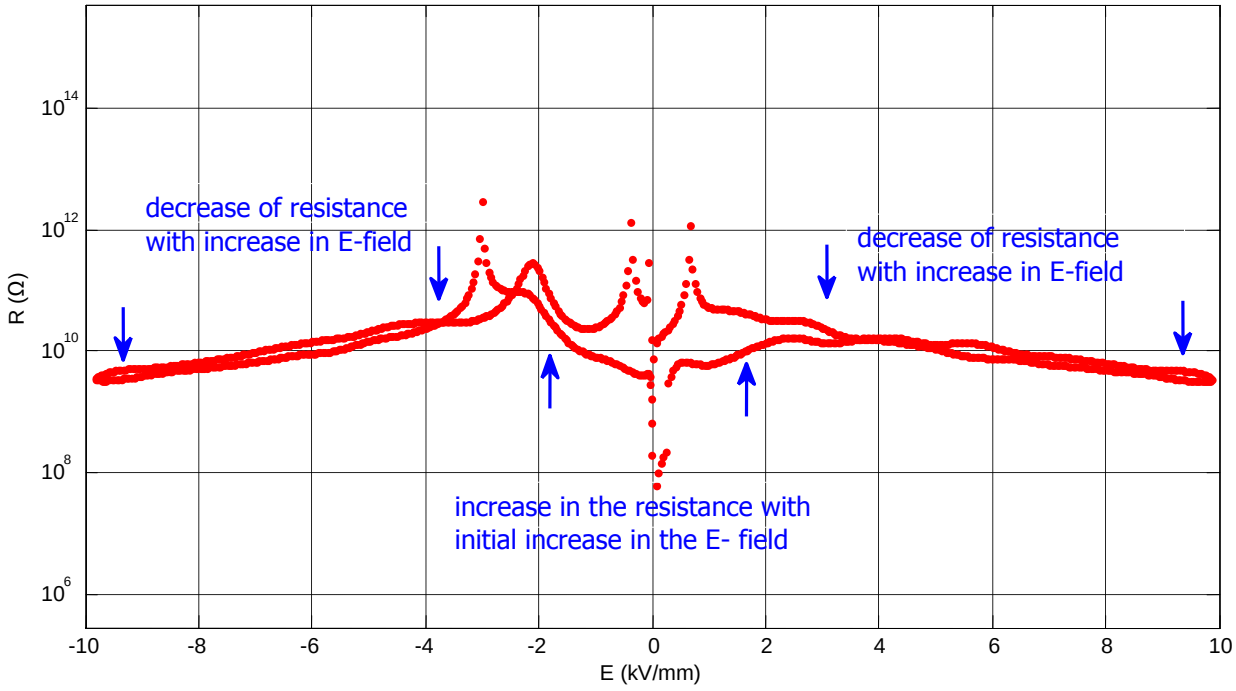

Figure 4-3 Field dependency of the resistance with increase in the Electric field with frequency of 0.1 Hz

The variation of the resistance of the insulating liquid with sustained electric field since it depicts the situation in real life transformers. A wide change in the in the conductivity at sustained fields is a parameter to be considered during the design stage to avoid excessive

stresses in either the paper or the oil. The results show a deviation of the resistance of the oil during the increasing half of each polarity from that during the decreasing half.

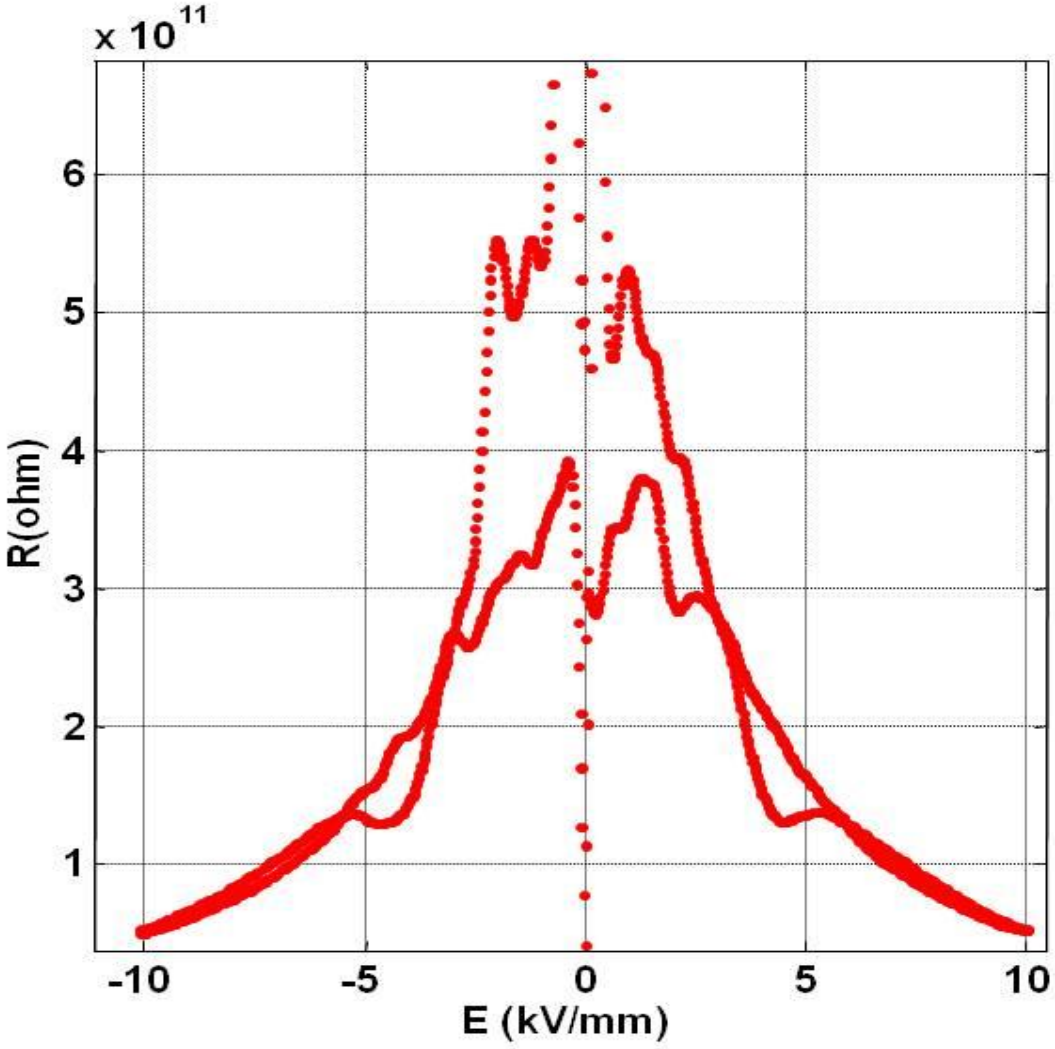

Figure 4-4 The resistance of the oil's dependence on the Electric field when a sinusoidal wave of frequency 0.01 Hz is applied

The Electric field dependency of the resistance when a sinusoidal field of maximum amplitude of 10 kV/mm and frequency of 0.01 Hz is applied to the oil sample is shown above. The results show a nearly symmetric alignment of the resistance values for both polarities and a further agreement to the previous results which has two regions of variation of the resistance. The results show an increase of the resistance for rte first 2 kV/mm field after which a reduction of the resistance with time is observed.

4.2 Time Dependency

The study of the variation of resistance with time evolution of the electric field is accomplished by a sustained stressing of the insulating oil within the test cell for long periods. In the experiments carried out in this work, the oil is stressed for periods up to twenty-four hours. In a bid to study the effect of time development alone without the effect of temperature variation, the work is carried out at room temperature with very little allowed variations. A constant amplitude and frequency of the applied voltage is also maintained.

The effect of the time evolution is studied mainly for sinusoidal input voltages at 0.01, 0.1 and 1 Hz.

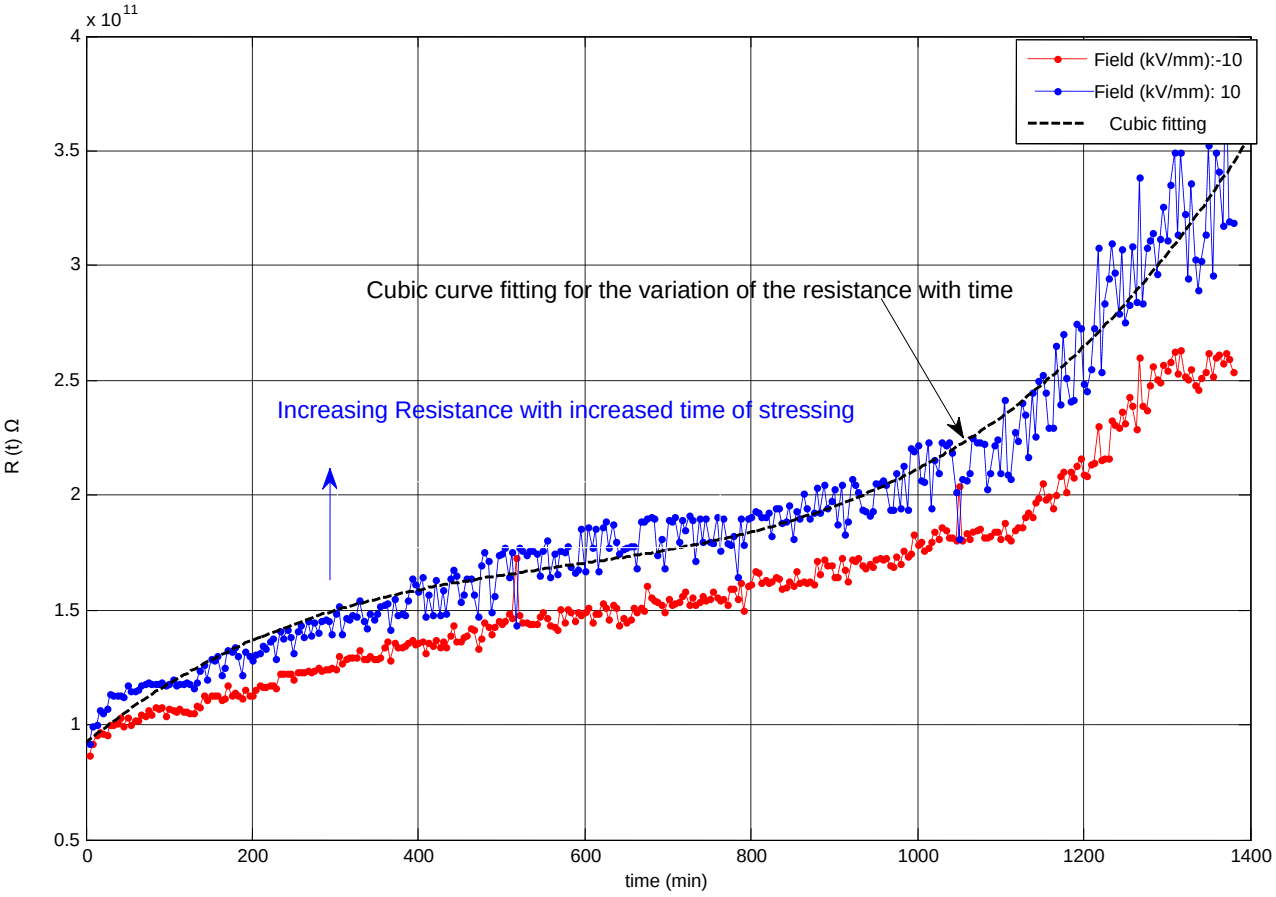

Figure 4-5 Time dependence of the resistance at an electric field of 10 kV/mm peak at a frequency of 0.01 Hz

The Figure 4-5 above shows the results obtained when a time evolution analysis is carried out on the resistance values obtained when the oil sample is stressed by a sinusoidal input voltage of frequency 0.01 Hz. The oil sample within the test cell is stressed for 1400 minutes keeping the voltage and temperature at nearly constant values. The resistance value obtained after the analyses of the results show that the resistance values at all stages of the sinusoidal input

wave decreases with time. In order to obtain a detailed knowledge on the development of the resistance with time, a selection of the variation at 10kV/mm is selected for detailed analysis, the result of which is shown above. The graph shows a monotonic increase of the resistance with time. The rate of increase is slower during the initial 600 minutes of stressing than the following time of stressing. The analysis examines the time evolution of both the positive and negative halves of the voltage. It is observed that the positive half shows slightly higher values of resistance for the whole period of the stress as compared to the negative half. A curve fitting of the positive half is done which shows a good cubic curve fitting. The negative half of the wave also shows a good cubic function fitting explain the widening of the difference between the positive and negative halves.

For the 1400 minute period, the resistance is increased over three folds for the positive half and a little over three and a half folds for the negative half.

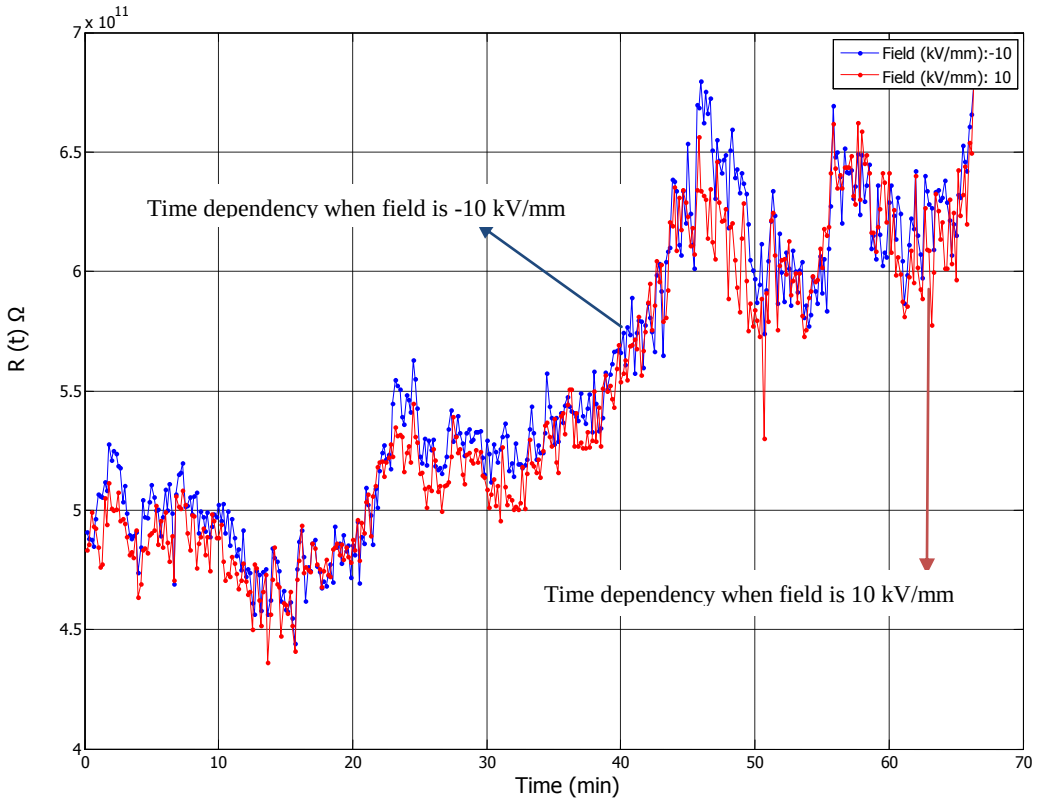

Figure 4-6 Time dependence of resistance at electric field strength of 10 kV/mm at 0.1 Hz

The diagram above shows the time dependence of the resistance of the oil with time of stress. There is a non-unilateral variation of the resistance throughout the total stress time. The resistance values increases and decreases with time but on the average, there is an increase of the resistance of the oil over the whole period of stress thereby agreeing with the results for the 0.01 Hz. The blue curve shows the results for the negative polarity field while the red curve show the time dependency for the positive half of the electric field.

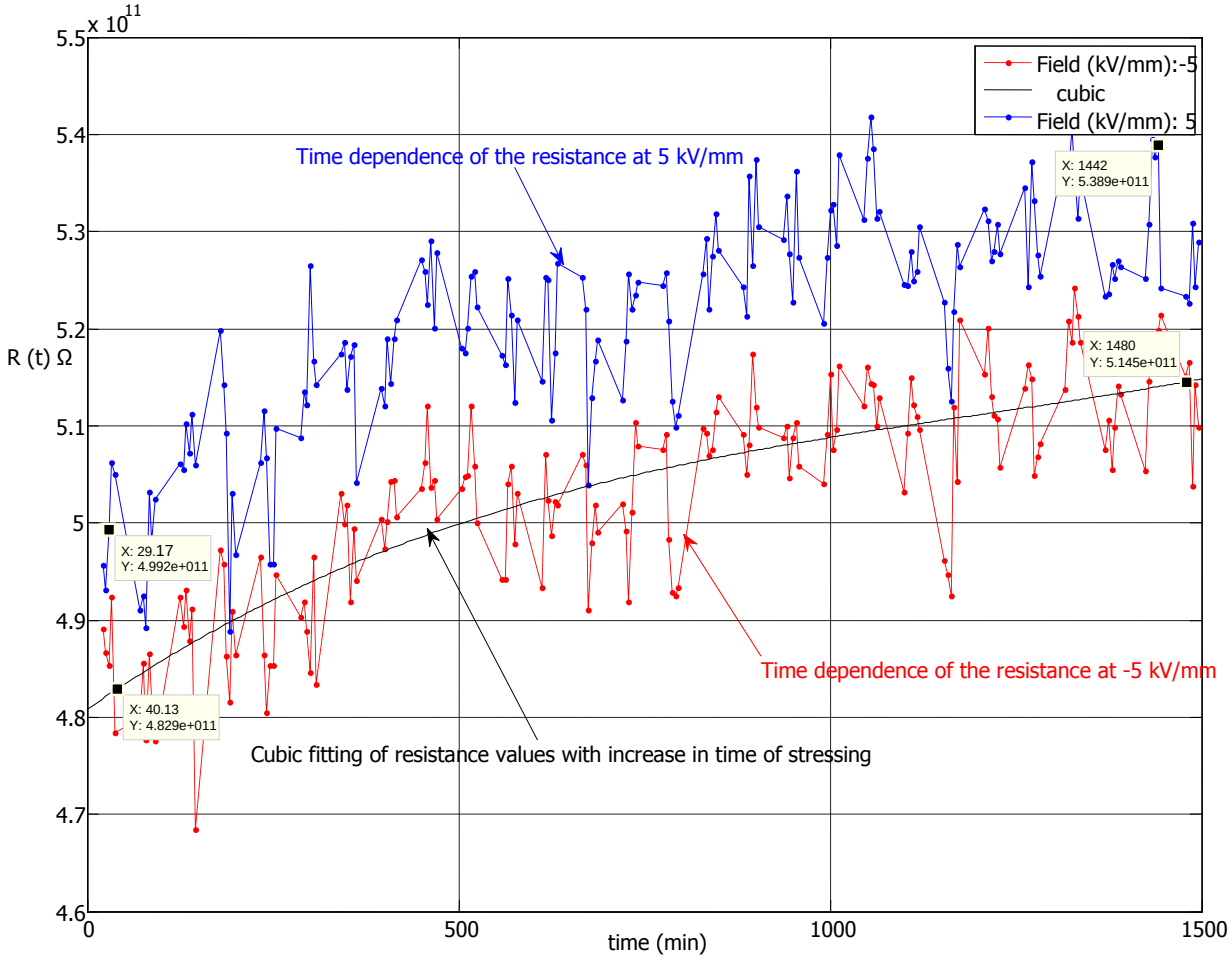

Figure 4-7 Graph of resistance against time of stress for an Electric field of 5 kV/mm for frequency of 0.01 Hz

The above diagram shows the time dependence of the resistance when the oil is stressed by 5kV/mm electric field. The resistance is seen to oscillate throughout the entire stress time but the general trend that emerges is the increase of the resistance with time. The resistance for the negative part of the electric stress at 40.13 minutes is $4.829 \cdot 10^{11}$ which is increased to $5.148 \cdot 10^{11}$ after 1410 minutes of stressing representing a 6.6% increase over the 1368.87 minutes of stress time. The resistance values for the positive polarity part of the electric field

shows values of comparably greater values though a minimal of 3.3% higher than the negative portion of the electric stress.

4.3 History and Pre-stressing

The effect of pre-stressing and history of the oil is studied in this section. The conditions under which the insulating oil has been and the treatment it has gone though prior to the measurement of the conductivity has been identified by researchers as an important factor that would indicate the value of conductivity that would be measured. In order to test this effect, conductivity analysis of the oil at two different conditions is carried out. In the first experiment, new oil is stressed with a 5kV/mm and frequency of 0.01 Hz sinusoidal electric field for 24 hours while the current is measured. The conductivity values are subsequently analysed. Afterwards, the same oil is stressed at half the previous electric field but at the same frequency and the conductivity is analysed from the measured current.

In the first experiment, it is seen from the result that the resistance values start at about $1.7 \cdot 10^{11}$ Ω for a peak electric field of 5 kV/mm and increases to $5.5 \cdot 10^{11}$ Ω after stressing for 1400 minutes. On the contrary the resistance values obtained during the stressing for a half the magnitude of electric field show a higher starting field of $4.8 \cdot 10^{11}$ Ω. This is shown in Figure 4-8.

One other observation and effect of the pre-stressing of the oil is the seemingly slower variation and of the resistance of the electric field with time. The resistance increases from $4.82 \cdot 10^{11}$ at the start of the stressing to $5.145 \cdot 10^{11}$ after 1500 minutes for the second experiment as opposed to the wider variation from $1 \cdot 10^{11}$ Ω at the start of stressing and $3.5 \cdot 10^{11}$ Ω at the end of 1400 minutes.

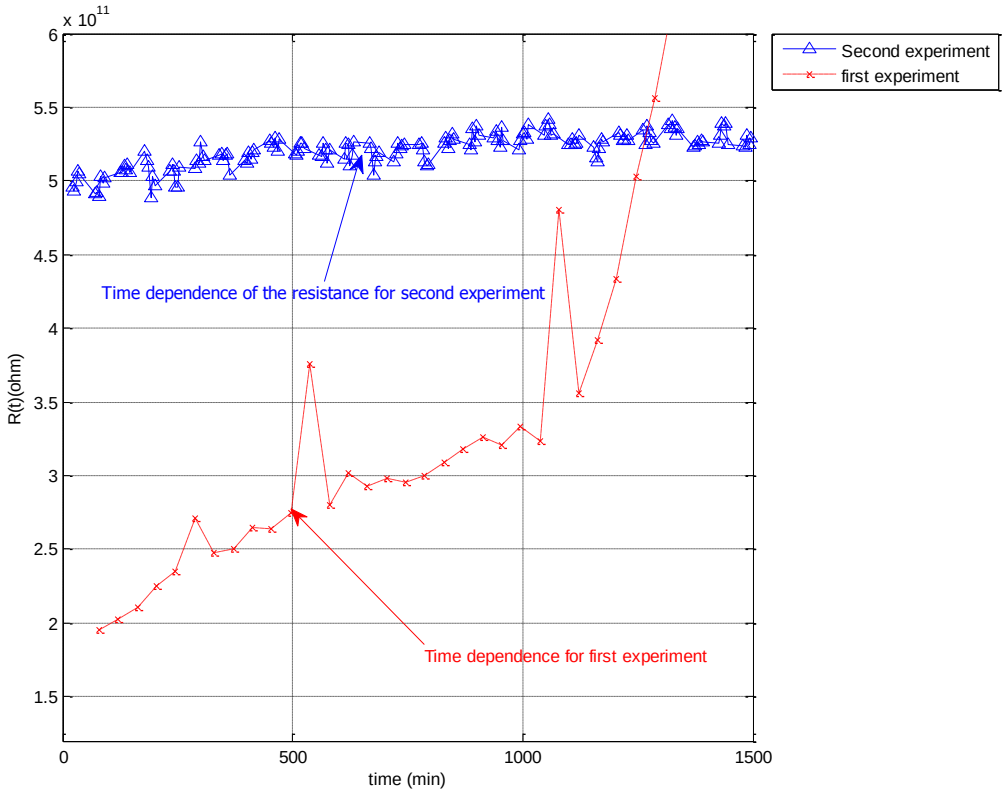

Figure 4-8 Effects of pre-stressing when electric field is maintained at 5kV/mm and frequency is 0.01 Hz

CHAPTER 5: COMSOL SIMULATIONS

In addition to the laboratory experiments carried out to investigate the conductivity of insulation oils at high fields, computer simulations using Comsol™ Multiphysics software is carried out to gain more knowledge on the variability of the conductance.

Comsol Multiphysics is commercial computer software that allows the modelling, specification of the physics, solving and visualisation of results from different physics problems. The advantage of this software is the ability to solve multiple physics problems simultaneously.

The software allows the definition of material, parameters, boundary conditions and physical partial differential equations to be solved what is the size of the screen. The focus of the simulation is to investigate the variation of the current, ion concentration with the variation of field and frequency.

5.1 The model

The most simplistic model is used for the work to limit complexities with boundary conditions. The test cell is simulated as a gap filled with oil and two straight boundaries. The model is a 2-dimentional cylindrical co-ordinate with one rotating field. There is the leverage of varying the length of the gap. Though the model is very simplistic, it is suffice to say it is just enough to get the most important information. To model the situation in the bulk oil, an assumption is made that there are positive and negative ions in the transformer oil. The ions and ion pairs are dissolved in the in the transformer oil, which can be considered to be a weak electrolyte. They can dissociate from a constant background concentration of ion pairs. These ions can both be transported in the electric field and recombined to form neutral molecules. In the oil, the majority of the ions are associated to ion pairs by electrostatic forces and only a few can dissociate to ions due to the low permittivity. The ions are dominant in the current transport of charge carriers. It is possible to use a simpler model where a one dimensional model.

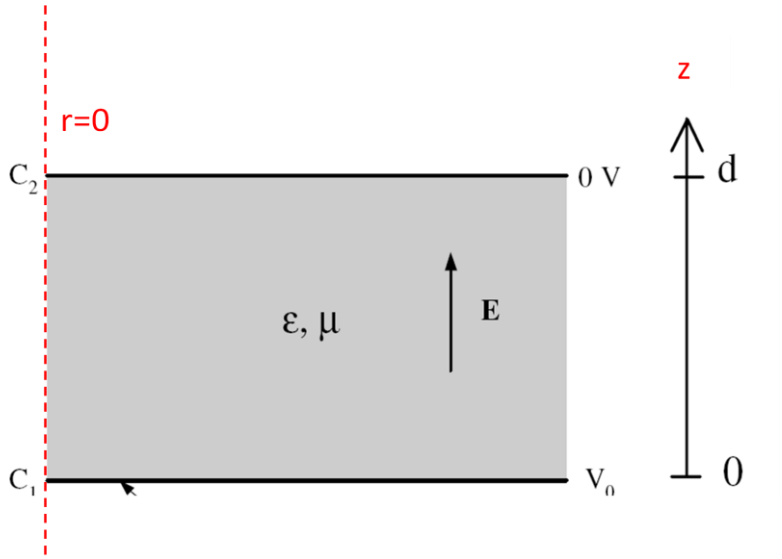

Figure 5-1 The Comsol model showing the two boundaries with metal electrodes(24)

The boundary conditions

There are four boundaries with this model, two of them as the interface between the bulk oil sample and the metal electrodes. The upper electrode is at a positive polarity voltage while the lower electrode is at a negative polarity of 20 kV.

Physics and Differential Equations

In carrying out the simulation two physics problems: electrostatics and convection and diffusion. The model utilises these two physics concurrently to simulate the combined effect of the electron and other charge carriers as well as the movement of these charge carriers.

Equations

The main goal is to calculate the resulting conduction current when gap is stressed with a high electric field. In order to achieve this, the ion diffusion drift model used by Uno Gävert et al.

With this model has a transport equation which defines the diffusion or convection of the charge carriers within the bulk of the oil as well the at the electrode interface. There is also the electrostatic equation which defines the charge carriers involved. Since the aim is to solve these equations simultaneously, a third equation is added to connect the previous two sets of equations. The current transport equations together with the continuity and Poisson's equation define the model mathematically.

Transport Equations

$$\begin{aligned} \partial p/\partial t + \nabla\left(\mu_p \vec{E} p - D_p \nabla p\right) &= S \\ \partial n/\partial t - \nabla\left(\mu_n \vec{E} n + D_n \nabla n\right) &= S \end{aligned} \qquad [5.1]$$

Diffusion constant

$$D_{p,n} = \mu_{p,n} \cdot kT/q \qquad [5.2]$$

Source Term

$$\begin{aligned} S &= k_D^0 cF(E) - k_R pn \\ k_R &= q\left(\mu_p + \mu_n\right)\big/\varepsilon_0\varepsilon_r \\ k_D &= k_D^0 F(E) = k_D^0 \cdot I_1\left(4b\right)\big/2b \\ k_D^0 &= k_R n_0^2/c \\ b &= \left(q^3 E/16\pi\varepsilon_o\varepsilon_r k^2 T^2\right)^{1/2} \end{aligned} \qquad [5.3]$$

Poisson equation

$$\nabla\cdot\left(\varepsilon_0\varepsilon_r\nabla\phi\right) = -q\left(p-n\right) \qquad [5.4]$$

$$\vec{E} = -\nabla\phi \qquad [5.5]$$

Where:

p is the positive charge carriers while n is the negative charge carriers

q is the elementary charge= 1.6021·10^{-19} C, k =1.3805·10^{-23}J/K (Boltzmann's constant)

k_D is the dissociation constant and k_D^0 is the dissociation constant at zero electric field

k_R is the Langevin recombination constant

D is the diffusion constant; E is the electric field

n_0 is the concentration of neutral ions in the bulk oil

F (E) is the field enhanced dissociation coefficient

I_1 is the modified Bessel function of the first kind

T is the temperature, k is Boltzmann's constant

In solving the above equations, initial conditions are set that the concentration of injected negative charges from the electrode is three times the initial concentration of charges in the bulk of the liquid. This initial guess saw originally use by ABB as a fitting parameter.

$$p_0 = n_0 = \sigma / q\left(\mu_p + \mu_n\right)$$
$$n_{inj} = 3 \cdot n_0 \qquad (24) \qquad [5.6]$$

Where:

σ is the conductivity

p_0 and n_0 are the initial concentration of positive and negative charge carriers respectively

n_{inj} the concentration of negative charge at the interface with the electrode

It is assumed that the background concentration of ion pairs is constant.

The calculation of the current is based on the total flux at the electrode. When a direct current is applied to the electrodes, it is observed that it takes a few seconds (about 0.8 seconds) for the conduction current to reach its steady state value. The calculated ion transit time; which s the time it takes anion to move from one electrode to the other corresponds with the time it takes the current to reach stable values.

In the electric field range utilised in the experiments, an assumption is made that electronic conduction is rather on the low side considering the fact the oil is new. As such, ionic conductivity which is brought about by the dissociation of neutrals is used for the calculation. Onsager's relation on the field enhanced dissociation is used in the calculation of the number of free ions available for conduction.

Homogeneity in the oil should mean that the ion concentration should be equal at any point in the bulk oil except close to the bare metal electrode where interface conditions would lead to a difference as a result of possible ion injection from the electrode. Interface conditions such as polarisation may lead to the increase in the capacitive current at high electric field.

5.2 Calculation of the Current

The total current is the sum of the two components: the conductive and the capacitive parts. The displacement current from the model is calculated by integrating the charges over the total surface area of the electrode. Since the charge density on the electrodes is equal to the value of the electric displacement field (D), the total charge is calculated as the integral of the electric displacement over the entire area. This follows from *Gauss law* which states that: *the electric flux through any closed surface is proportional to the enclosed electric charge.*

$$Q = \int 2\pi r D_{es} \cdot dl \qquad [5.7]$$

Where D_{es} is the electric displacement field

The capacitive current is then calculated from the total charge as the differential of the charge with time.

$$I_{disp} = \frac{dQ}{dt} \qquad [5.8]$$

The conductive part of the current is calculated as the integral of the net drift of charges over the area.

$$I_{cond} = \int q \cdot 2\pi r(ntflux \cdot c - ntflux \cdot c_2) \cdot dl \qquad [5.9]$$

Once the conductive current is calculated, it is added to the capacitive current calculate from the displacement current to get the total current

$$I_{total} = I_{disp} + I_{cond} \qquad [5.10]$$

In order to derive the actual conductive current, the Laplacian capacitive current is subtracted from the total current to obtain the actual conductive current.

5.3 Results

The conduction current obtained from the simulation when the frequency is 0.1Hz, peak voltage of 20 kV is shown below.

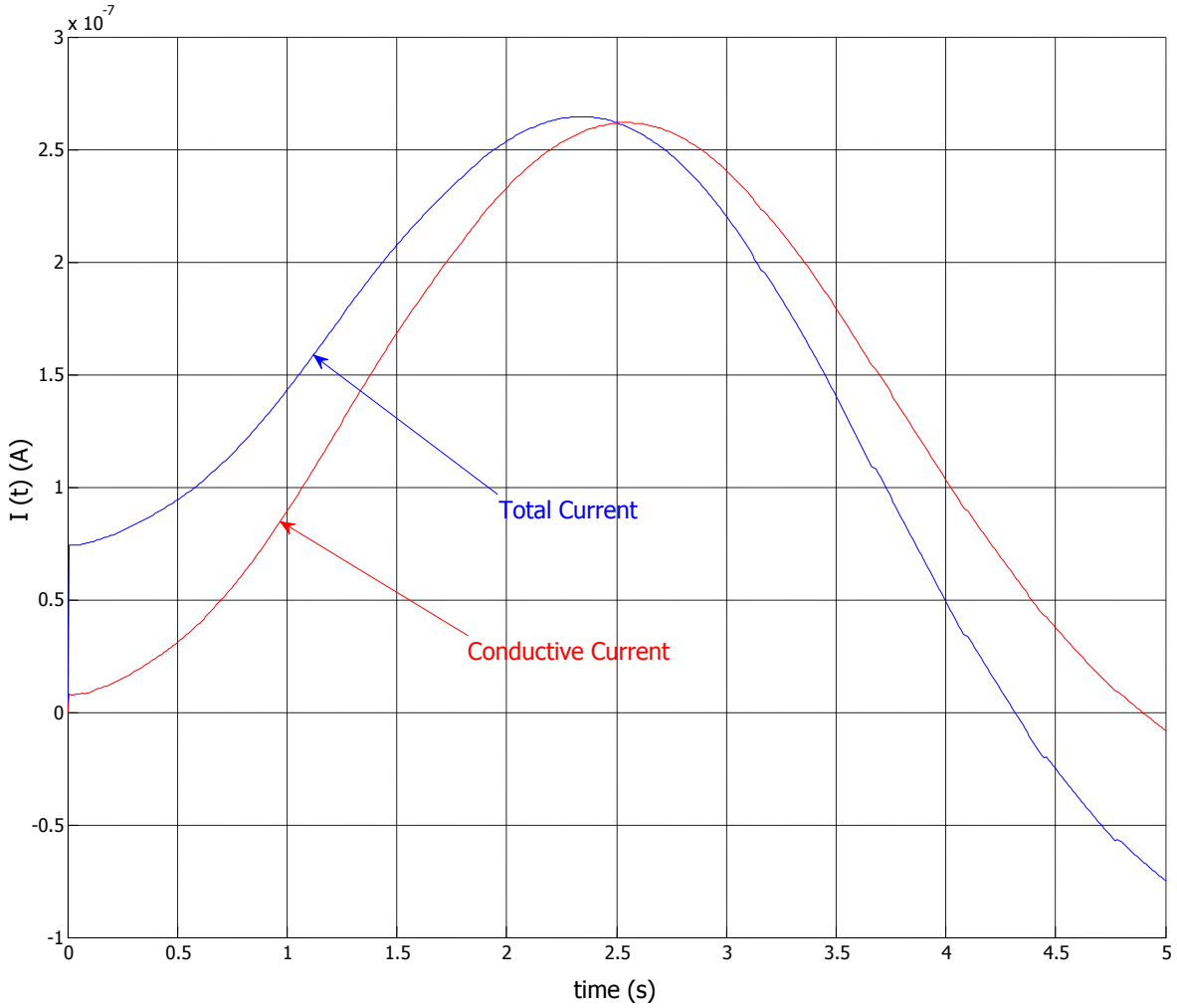

Figure 5-2 Conductive and total current at an E-field of 10 kV/mm and frequency of 0.1 Hz for half a period

After the running the Comsol Script with the necessary parameters, the conductive and total current are plotted together as shown in the Figure 5-2. The conductive current in blue follows a near sinusoidal wave shape with peak of $2.7 \cdot 10^{7}$ Amperes. The difference between the total current and the conductive current represents the capacitive current.

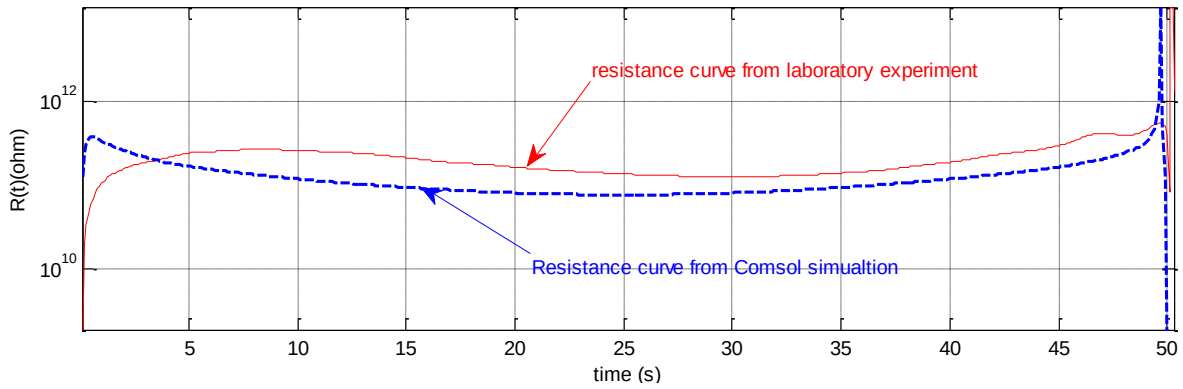

Figure 5-3 Graph of resistance when the electric field is 10 kV/mm and the frequency of 0.01 Hz

The graph of the resistance of the oil when stressed by a 10 kV/mm peak sinusoidal peak electric field is shown in the figure above. The resistance shows very little variation in amplitude throughout the entire half period considered. It has its lowest value of $7 \cdot 10^{10}$ at the maximum point of the input voltage and highest resistance close to the zero crossing of the input voltage..

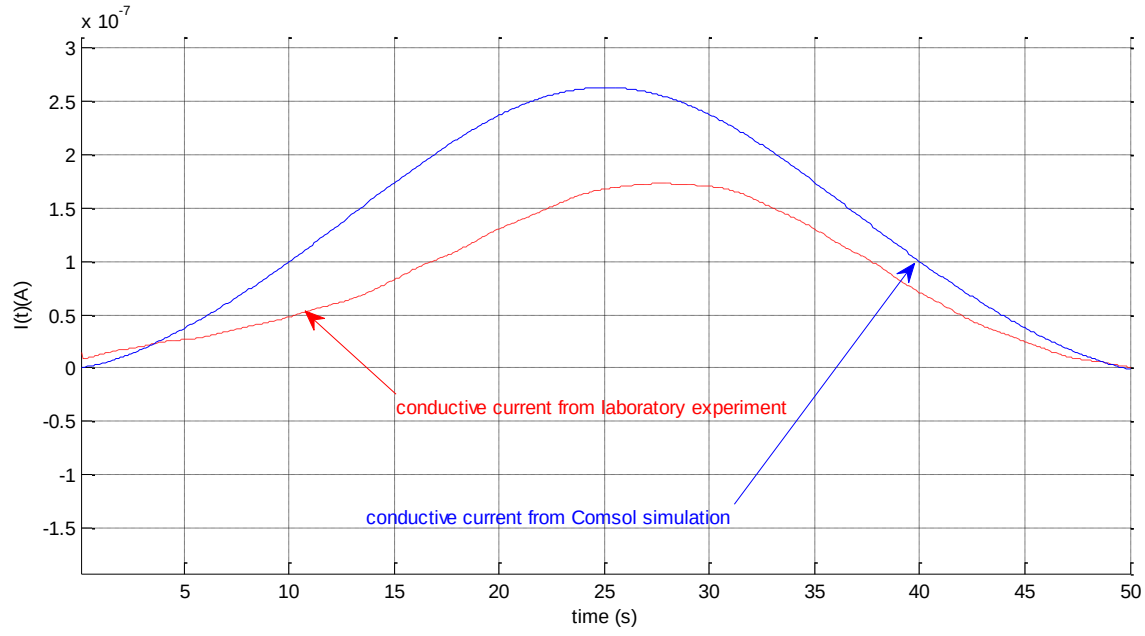

Figure 5-4 Comparing conductive currents from the laboratory experiment to that obtained from the Comsol simulation when field is 10 kV/mm and frequency is 0.01 Hz

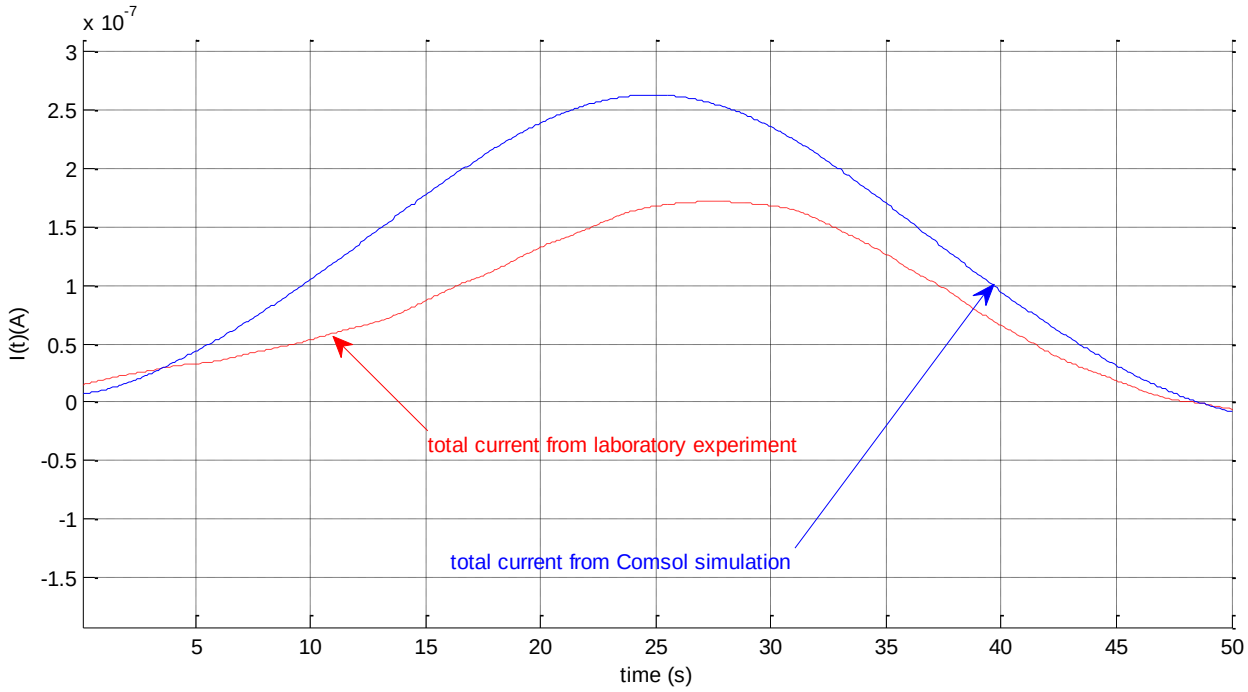

Figure 5-5 Comparing the total currents obtained from the laboratory experiment to that obtained from the Comsol simulations when electric field is 10 kV/mm and frequency is 0.01 Hz

The Figure 5-4**Error! Reference source not found.** shows conductive current results of both the Comsol simulation and the laboratory experiment when the applied voltage over the 2 mm gap is 20 kV and the frequency is 0.01 Hz. There is similarity between the current curves observed difference but a difference in the amplitudes. While the Comsol simulation show a peak of $2.7 \cdot 10^{-7}$ A, a lesser value of $1.789 \cdot 10^{-7}$ A is obtained showing a reduction of $0.911 \cdot 10^{-7}$ A.

The total conduction current from the Comsol simulation is calculated from the total flux of charge at the electrodes. The calculated by the total flux linkage at the electrode. The Figure 5-5 shows the total current values obtained from the laboratory experimental results and that from the comsol simulations for an electric field of 10 kV/mm and frequency of 0.01 Hz. There is a clear similarity between the two curves in terms of the shape.

It is clear from these results that the Comsol simulation gives results that can be fairly fit the results from the laboratory results but for slight difference in the magnitudes.

CHAPTER 6: DISCUSSION

Inferring from the current waveforms, it is clear that the total current reduces with decreasing frequency of the applied voltage though the amplitude is kept constant. The total current is a sum of the conduction current and the capacitive current. With a constant gap distance between the electrodes and an approximately unchanging permittivity, the capacitive reactance becomes a function of the frequency of the waveform.

$$X_c = {}^{-j}\!\!\diagup\!\!_{2\pi f \cdot C} \qquad [5.11]$$

Where, f is the frequency of the input voltage while C is the capacitance of the gap.

A reduction of the frequency of the input waveform, the capacitive reactance is increased and a resulting decrease of the capacitive current is observed ($I_c = V/X_c$). This reduction of the capacitive current creates a challenge in the correct measurement.

The triangular wave method which was originally used by ABB in the measurement of the conductivity of insulating oils was very efficient and convenient method to measure conductivity. Unfortunately, this method was found to less efficient at higher field strengths. The triangular wave was originally used with peak voltage of 10 V as such falling within the initial Ohmic region of conduction; where ions are replaced as soon as they drift away in the bulk of the oil. As the electric field is increased beyond the ohmic region, the inefficiency of the triangular wave becomes evident.

6.1 Time Dependency

Short-term conductivity is relatively high because of the presence of ions; long-term conductivity is given by a new equilibrium of ion generation and recombination: moderate fields strengths reduce the number of existing ions while a further increase in the field result in the generation of new charge carriers. The results of the time dependence calculation and the resulting graphs show a general trend of decreasing conductivity with an increase in the time of stress. The Figure 4-5 on page 32 shows the time dependence of the resistance with increasing time of stress when a 10kV/mm electric field is applied across the electrodes. The monotonic increase of the resistance with time under both polarities of electric field suggests an ongoing internal mechanism that either reduces the number of charge carriers available for conduction, the cleansing of the oil or a process that recombines the dissociated ion pairs. The increase which is a little more than 2.5 times the resistance at the start of the stress as it is

after 1400 minutes show a rather wide variation considering that the temperature was kept at an almost constant value throughout the duration of the stress. The variation is somewhat less in the recurring experiments using the same oil. The resistance variation with time of stress an electric field of 5kV/mm was applied across the electrode shows a similar monotonic increase of the resistance with time but at a lower 6.6% after the oil is stressed for 1500 seconds. Another interesting observation is the value of initial resistance measured under both experiments. In the experiment using an electric field of 10kV/m, the initial resistance measured was a minimum $1 \cdot 10^{11}$ Ω while it is $4.8 \cdot 10^{11}$ Ω for the 5kV/mm stress. This trend could be explained by the fact that the second measurement though of a half the stress of the first one , was carried out on the same oil after the initial measurements with 10kV/mm with a very long stress time resulting the start of the stabilisation of the conductivity of the oil. This is also evident in the nominal 6.6% increase in the resistance value after a 1500 minute stress under 5 kV/mm.

6.2 Electric Field Dependency

The direct relationship between electric field and conductivity value is very evident in the results of the experimental work carried out in this work. The graphs of resistance against electric field for the various frequencies show the general trend of incremental change in the resistance with electric field up to between 1-3 kV/mm. This is comparable to values reported in literature (8)(9). The initial increase of the resistance with time could be explained by the sweeping away of charge carriers at a faster rate than they are produced within the bulk of the oil. It is reported in the literature than field enhanced ionic dissociation is not in operation at this stage. The decrease of the resistance with increase of the electric field that occurs after the threshold of between 1 and 3 kV/mm represents a rapid increase in the free ion concentration within the bulk oil due to the to the production by electric field enhanced dissociation (17). Since the experiments are carried out at an almost constant temperature, the increase in the conductivity could not be explained by the increase in the mobility and hence the velocity of the charge carriers but rather on the generation of more charge carriers by a number of different mechanisms. Since the electrodes used in the experiments were uncovered, the possibility of electron injection from the electrode cannot be ignored though the level of electric field intensity utilised in the various experiments are not so high to produce an avalanche of electron emission from the cathode. Nevertheless, due to the imperfect nature of the electrodes and the asperities on the electrode surface, current filaments from the electrodes

cannot be ignored. On the contrary, the possibility of field-enhanced dissociation is high due to the rather lower voltage level at which it starts (14).

6.3 Comsol Simulation

In conducting the simulation with Comsol multiphysics, an assumption of a uniform electric field is used. A way to explain this is to study the quotient of the transition time of the ion through the gap ($\tau_{transit}$) and the dielectric relaxation time (τ_{relax})

$$\kappa = \frac{\tau_{transit}}{\tau_{relax}} \qquad [5.12]$$

where

$$\tau_{transit} = \frac{d}{\mu U / d} \qquad [5.13]$$

$$\tau_{relax} = \frac{\varepsilon_0 \varepsilon_r}{\sigma} \qquad [5.14]$$

For small values of κ (<< 1), the ions are transported through the oil gap before they relax. The sweep out of the ions gives an almost uniform electric field. Therefore for a small gap stressed with high voltage as used in the experiments, the relative field distortion is small and it suffices to say it is uniform.

Comparing the results obtained from the Comsol simulation to that from the experiments, it is observed that the conductive current is kept at an almost constant magnitude for all frequencies in the Comsol simulation while there is difference in the values in the laboratory set up. Frequency dependency of

The results of the simulation shows the near reproducibility of the conduction currents when the sinusoidal wave is applied to the electrodes. The infinitesimal discrepancy in the magnitudes which is the range of 2 – 3 could be attributed to the incorrect modelling of the ion concentration at the electrode which is injected into the bulk ion from the electrodes. In the simulation a concentration of three times the neutral ion concentration is used as the free ion concentration at the electrode surface; this choice is arbitrary and only a fitting parameter. The difference could also be attributed to the challenge in clearly and correctly defining the boundary conditions for the model.

CHAPTER 7: CONCLUSIONS

The results of the laboratory experiments conducted throughout this work show a clear dependence of the conductivity of the oil on the input supply voltage used in the experiment and that the variation of the conductivity is not monotonic from zero electric field to the maximum but in the contrary show two clear regions of change: an initial decrease in the value of the conductivity with increasing field up to fields of 2 kV/mm and a subsequent increase in the conductivity with increasing electric field.

Inferring from the results obtained and the literature, it is difficult to attribute the increasing conductivity after 2-3 kV/mm to a particular phenomenon. The conductivity of the oil is observed to increase by up to 2 decades magnitude during the period of increasing the electric field from 2.7 kV/mm to 10 kV/mm Since the electrode used in the experiments were bare and has regions of asperities, charge injection from the bare electrode cannot be ignored. As such there is likely to be two high voltage conduction phenomena taking place simultaneously: Electric field enhanced dissociation and Field injection.

The duration which the oil sample is stressed under the electric field has a great impact on the value of conductivity that is measured. It is clear that a higher duration of the time of stress deduces the conductivity up to 3 times the magnitude after 24 hours as compared to that at the initial stress time. As such the use of the IEC 61620 for the measurement of the conductivity does not give a true reflection of conductivity values of oil in a transformer which is under long periods of stress.

The rate of deduction of the conductivity of the oil sample for long stress times reduces and approaches a stable value after 50 hours of stress. This shows that the true DC conductivity can be approached when enough time of stress is used in the experiments. However the required time needed to reach this value is not definite.

The use of both the triangular and sinusoidal waveforms in the experiments gave good results but for the numerical challenges in computing the resistance values from the triangular wave method.

The results from the experiments can fairly be reproduced by a simulation in Comsol Multiphysics though there are variations in the magnitudes of the resistance and currents as compared with actual experimental results. The variations are likely to be the effect of the

inability to correctly model the interface conditions and all material properties correctly. The model used had a minimum number of parameters for fast and easy simulation.

The conductivity as a parameter of the insulating oil is not a constant but varies on wide range depending on the electric field, temperature, stress time, history and pre-stressing and a little extent on the frequency. The values thus obtained from the various experiments therefore do not indicate exact values but rather apparent conductivities for the instantaneous conditions of the experiment.

Since the conductivity of the oil shows a wide range of variation compared to that of the pressboard in transformers, the pressboard must be dimensioned to sustain the varying dc component of the electric field unlike the in the power frequency (AC) case where there is less variation in magnitude of the permittivities of both the oil and pressboard.

REFERENCES

1. **R Bärsch, A Küchler.** *Stressing and electrical behaviour of insulating systems at dc streses and mixed stresses.* Cologne : s.n., 2010.

2. **Tortai, J.H., Bonifaci, N., Denat, A.** Insulating Properties of Some Liquids After an Electric Arc. *IEEE Transactions on Dielectrics and Electrical Insulation.* February 2002, ss. 3-9.

3. **Ingebrigtsen, Stian.** *The Influence of Chemical Composition on Stremaer Initiation and Propagation in dielectric Liquids.* Trondheim : Phd Thesis, NTNU, Norway, 2008.

4. *On the Measurement of the Conductivity of Highly Insulating Liquids.* **R Tobazéon, J. C. Filippini and C. Marteau.** 1994, Dielectrics and Electrical Insulation, IEEE Transactions, ss. 1000-1004.

5. *Modeling and Measurement of Electric Fields in Composite Oil/Cellulose Insulation.* **Uno Gäfvert, Olof Hjortstam, Yuriy Serdyuk, Christer Tørnkvist and Lars Walfridsson.** s.l. : IEEE Explore, 2006. Conference on Electrical Insulation and Dielectric Phenomena. ss. 154-157.

6. *The Conductivity of Insulting Oils.* **J B Whitehead, R H Marvin.** 19, s.l. : AIEE, 1930, Vol. 30.

7. **E Kuffel, W S Zaengl, J Kuffel.** *High Voltage Engineering:Fundamentals.* s.l. : Elsevier, 2008. ISBN:978-0-7506-3634-6.

8. *Insulation Problems in HVDC-Converter Transformers.* **Lampe, P Hessen and W.** ss. 30-44.

9. **Wahlstrøm, Bo.** Voltage Tests on Transfomers and Smoothing Reactors for HVDC Transmission. *Electra.* 46.

10. *Simple Method for Determining the Electric Conductivity of Dielectric Liquids.* **Uno Gäfvert, Håkan Kols and Janez Marinko.** ss. 23:1 - 23:5.

11. *Ion Injection in Hydrocarbons.* **A. Denat, B. Goose and J. P. Goose.** 1979, Journal of Electrostatics, ss. 205-225.

12. *Theory of High-Field Electric Conduction and Breakdown in Dielectric Liquids.* **Kao, Kwan C.** 1976, IEEE Transaction on Electrical Insulation, ss. 121 - 128.

13. *High-Field Conduction in Dielectric Liquids Revisited.* **Felici, N.** 1985, IEEE Transaction on Electrical Insualtion, ss. 233 - 238.

14. *A Tentative Explanation of the Voltage-Current Characteristics of Dilectric Liquids.* **Felici, N J.** s.l. : 12Elsvier Scientific Publishing Company, 1982, Journal of Electrostatics, ss. 165-172.

15. *Electro-convection in a dielectric liquid layer subjected to unipolar injection.* **J C Lacroix, P Atten, E J Hopfinger.** 3, s.l. : Jounal of Fluid Mechanics, 1975, Vol. 69, ss. 539 - 563.

16. *Electric Field Distribution in Transformer Oil.* **Uno Gäfvert, Albert Jaksts, Christer Tørnkvist and Lars Walfridsson.** s.l. : IEEE Explore, 1992. IEEE Transaction on Electrical Insulation. ss. 647-660.

17. *Deviations from Ohm's Law in Weak Electrolytes.* **Onsanger, Lars.** 9, s.l. : AIP, 1934, Vol. 2. ISSN 10897690.

18. **Lewis, T J.** The electric strenght and high field conductivity of dielectric liquids. *Progress in Dielectrics.* 1959, Vol. 1, ss. 97-140.

19. *D. C. conduction in liquid dielectrics, Part II-Electrohydrodynamic phenomena.* **Felici, N J.** 1972, Direct Current, Vol. 2, ss. 147 - 165.

20. **Commission, Internationa Electrotechnica.** IEC 61620. *Insuating Liquids; Determination of the dielectric dissipation factor by measurement of the conductance and capacitance ; Test method.* 1998.

21. **Commission, International Electrotechnical.** IEC 60247. *Insulating Liquids; Measurement of relative permittivity, dielectric dissipation factor(tan d) and d.c. resistivity.* 2004.

22. **Uno Gäfvert, Håkan Kols, Janez Marinko.** *Simple Method for Determining the Electric Conductivity of Dielectric Liquids.* Västerås : s.n.

23. *Influence of Oil Quality on Field Distortion in Transformer Oil Under DC Stress.* **Uno Gäfvert, Håkan Kols and Janez Marinko (ASEA Research and Innovation).** ss. 278-286.

24. *Finite element analysis of charge injection and transport in a dielectric liquid.* **S.-H. Lee, F. O'Sullivan, I.-H. Park, M. Zahn, L. Pettersson, R. Liu, O. Hjortstam, A. Jaksts, T. Auletta, and U. Gafvert,.** Piscataway : s.n., 2006. IEEE.

25. *Emperical Treatment of High Field Conduction.* **Zoledziowski, S.** Bath : IEEE, 1996. Intation Conference on Dielectric Materials, Measurement and Applications. ss. 82 - 85.

26. *Insulation Problems In Power Transformers for HVDC Transmissions.* **Z. M. Beletsky, V. G. Butkevich,A. K Lokhanin, E. L. Topoliansky and I. D. Voevodin.**

27. *High Field Conduction in Dilectric Liquid with Ramped Voltage Application: A theory of the Mechanism.* **Watson, Alan.** Grenoble : IEEE, 1990. International Conference on Dielectric Liquids. ss. 156 - 160.

28. *A High-Accuracy, Calibration-Free Technique for Measuring the Electrical Conductivity of Liquids.* **Susan L. Schiefelbein, Naomi A. Fried, Kevin G. Rhoads and Donald R. Sadowayc.** 1998, Review of Scientific Instruments, ss. 3308-3313.

29. *On the Measurement of the Conductivity of Highly Insulating Liquids.* **R. Tobazéon, J. C. Filippini, C. Marteau.** 6, Baden-Dattwil : IEEE Dielectrics and Electrical Insulation Society, 1994, Vol. Volume 1. 1070-9878.

30. **Nosseir, Abdel-Razak.** Effect of Dissolved Gases, Stress and Gap Spacing on High-Field Conductivity in Liquid Insulants. *IEEE Transaction on Rlectrical Insulation.* June 1975, ss. 58 - 62.

31. **Instruments, Irlab.** Irlab Company. *Irlab Instruments Website.* [Internett] 2002. [Sitert: 26 October 2010.] http://www.irlab.fr.

32. *Modeling the Effect of Ionic Dissociation on Charge Transport in Transformer Oil.* **Francis O'Sullivan, Se-Hee Lee, Markus Zahn, Leif Pettersson, Rongsheng Liu, Olof Hjortstam, Tommaso Auletta, Uno Gafvert.** Kansas City, Missouri : IEEE, 2006. IEEE Conference on Electrical Insulation and Dielectric Phenomena. ss. 756-759. ISBN 1-4244-0547-5.

33. *On the role of temperature and impurities in the low field conduction of insulating liquids.* **Diabi, R., et al.** Roma : IEEE, 1996. International Conference in Dielectric Liquids. ss. 350-353.

34. *High Field Conduction and Prebreakdown phenomena in Dielectric Liquids.* **Denat, A.** s.l. : IEEE, 2005. International Conference Dielectric Liquids. ss. 57 - 62.

35. **A. Kuechler, F. Huellmandel, K. Boehm, M. Liebschuner, Ch. Krause andB. Heinrich.** *Parameters Determining the Dielectric Properties of Oil Impregnated Pressboard and Presspaper in AC and DC Power Transformer Applications.* Ljubljana, Slovenia : Internation Symposium onHigh Voltage Engineering, 2007.

36. *Impact of dielectric material responses on the performance of HVDC power transformer insulation.* **A. Kuechler, F. Huellmandel, J. Hoppe, D. Jahnel, C. Krause, U. Piovan and N. Koch.** Schweinfurt, Germany : s.n.

37. *Electrical Conduction of Solutios of An Ionic Surfurcant In Hydrocarbons.* **A. Denat, B. Gosse, J. P. Gosse.** 1982, Journal of Electrostatics, ss. 197-205.

38. *Conduction of Electricity by Dielectric Liquids at High Field Strengths.* **Plumley, H J.** 2, Chicago : Physical Review, 1941, Vol. 59.

39. *Modeling and Measurement of Electric Fields in Composite Oil/Cellulose Insulation.* **Uno Gäfvert, Olof Hjortstam, Yuriy Serdyuk, Christer Tørnkvist and Lars Walfridsson.** s.l. : IEEE Explore, 2006. Conference on Electrical Insulation and Dielectric Phenomena. ss. 154-157.

40. *Initial Recombination of ions.* **Onsager, Lars.** 1938, Physical Review, ss. 555 - 557.

41. **Milan Saravolac and Cigre JWG A2/B4-28.** *HVDC Transformers-Design Review Test Procedures and Reliability in Service.* Paris : Cigre, 2006.

42. *Space-Charge and Field Distribution In Transformers Under DC Stress.* **Uno Gäfvert, E Spicar.** Paris : Cigre, 1986. Intrenational Conference on Large High Voltage Electric Systems. ss. 12.04(1-4).

APPENDICES

Appendix 1: Current , Voltage and Resistance plots for a 1 Hz 10kV/mm triangular field

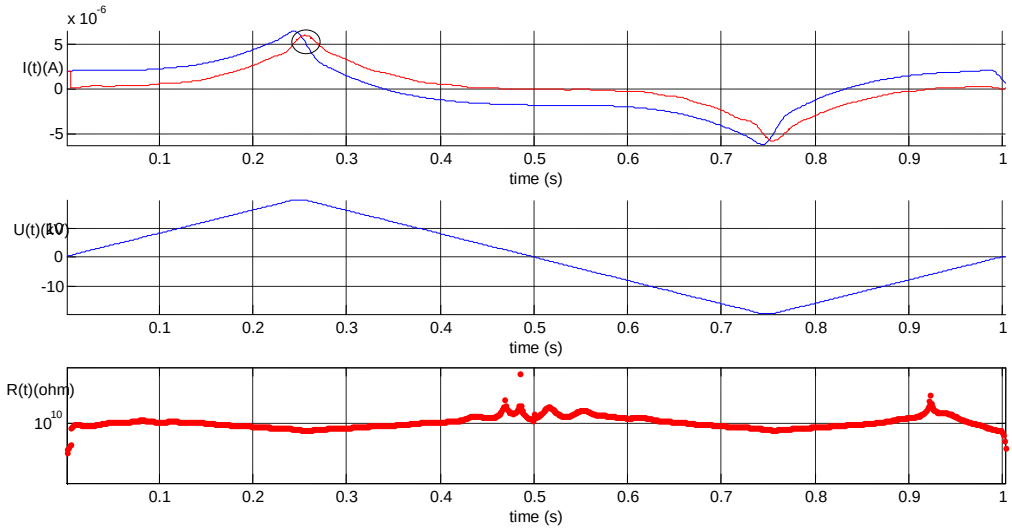

Appendix 2: Field dependence of resistance for 1hz 10 kV/mm triangular field

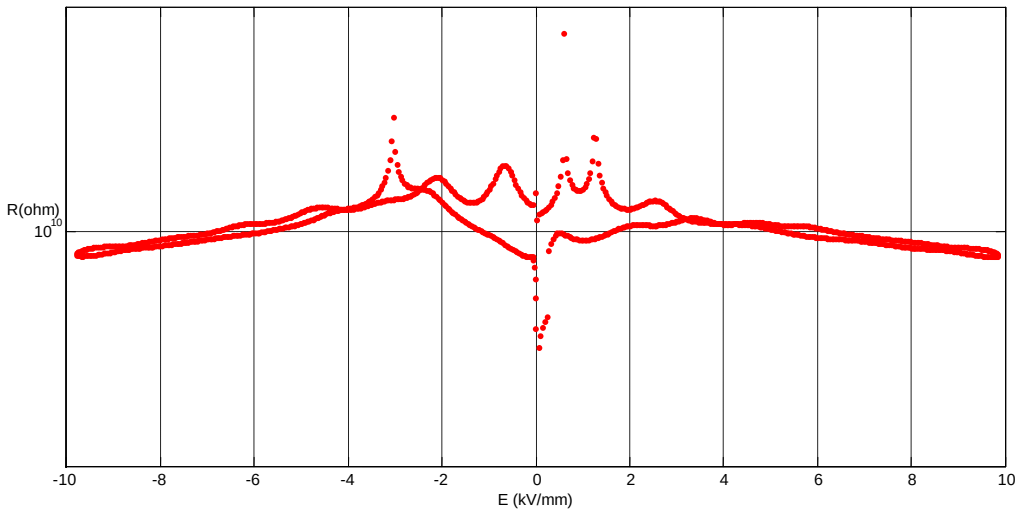

Appendix 3: LabView Programme

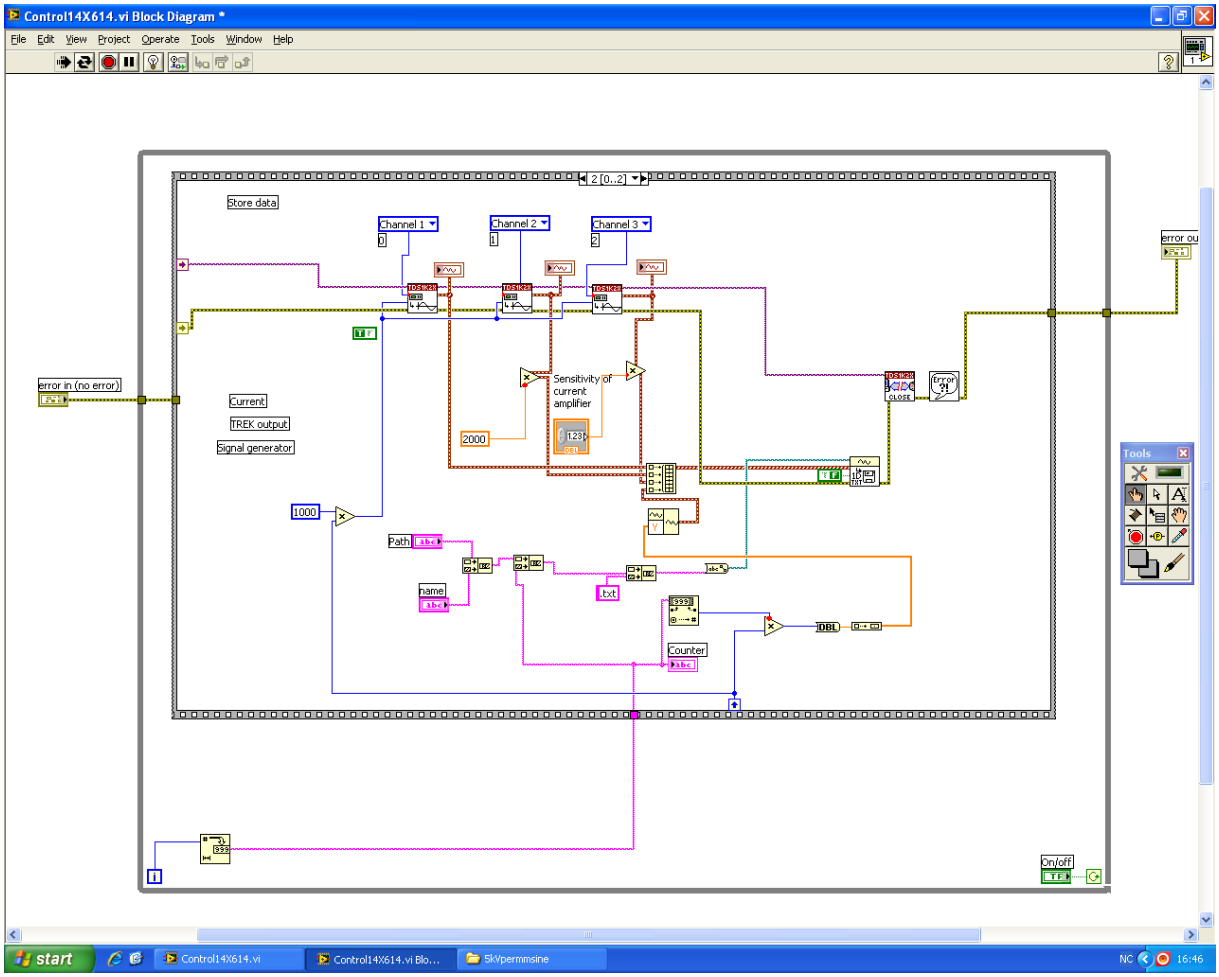

Appendix 4: Matlab Script for Analyzing and Plotting the Results

```
clear all;
close all;

%%%%%%%%%%%%%%%%%%%%%%%%%%%%%%%%%%%%%%%%%%%%%%%%%%%%%%%%%%%%%%%%
%%%%%%%%%%%%%% definition of constants %%%%%%%%%%%%%%%%%
%%%%%%%%%%%%%%%%%%%%%%%%%%%%%%%%%%%%%%%%%%%%%%%%%%%%%%%%%%%%%%%%
scrsz=get(0,'ScreenSize');                                  % screen
size
maxWindow=[1 31 scrsz(3) scrsz(4)-104];
Param.eps0 = 8.84*10^(-12);                                 % vacuum
permitivity
Param.e = 1.6 * 10 ^(-19);                                  % electron
charge (C)
```

```
Param.epsR = 2.2;                                          % relative
permittivity oil
Param.d = 2e-3;                                            % gap
distance (m)
Param.D = 9e-2;                                            % plane
electrode diameter
Param.A = pi*(Param.D/2)^2;                                % plane
electrode area
Data.NumAvg = 10;                                          % number of
files to average over
Data.Recordlength = 2500;

Data.I = (0);
Data.U = (0);
Data.UC = (0);
Data.dt = (0);                                             % (s)
Data.t = (0);                                              % (s)
Data.t = (0);
Data.I_C = (0);
Data.R = (0);
ZeroCross = (0);

%%%%%%%%%%%%%%%%%%%%%%%%%%%%%%%%%%%%%%%%%%%%%%%%%%%%%%%%%%%%%%%%
%%%%%%%%%%%%%      selecting data     %%%%%%%%%%%%%%%%
%%%%%%%%%%%%%%%%%%%%%%%%%%%%%%%%%%%%%%%%%%%%%%%%%%%%%%%%%%%%%%%%

[fn, pathname] = uigetfiles('*.txt','J:\Prosjekt\Avd14\14X614 HVDC Oil
Conductivity\Measurements\2011-04-
05\10kVpermmsine0.01hz\10kVpermmsine0.01hz\');
iii = 0;
for ii = 1 : Data.NumAvg : length(fn)
   I = (0); U = (0); UC = (0); dt = (0); t = (0); Data.UsedRecordlength
= (0);
   iii = iii + 1;
   for n = 1 : Data.NumAvg
     if n+ii-1 < length(fn)
       y = (0);
       [y,dt,t] = ReadColData14X614(fullfile(pathname,fn{n+ii-
1}),Data.Recordlength);
```

```
        n+ii-1
        name = fn{n+ii-1};
        p = (0);
        mm = 0;
        Data.f_nyquist = 1/(2*dt);
% Nyquist frequency
        Param.f_cut = Data.f_nyquist/15;
% Hz
        Wn = Param.f_cut/Data.f_nyquist;
        [b,a] = butter(3, Wn, 'low');
% 3rd order Bütterworth low-pass filter to supress high frequencies
        y(:,2) = filtfilt(b,a,y(:,2));
        % find zero-crossings and selects one period of signal
        for m = 4 : 3: Data.Recordlength
                if sign(y(m,2))== 1
                   if sign(y(m-3,2))<1
                     mm = mm + 1;
                     p(mm) = m;
                   end
                end
        end
        ZeroCross(ii) = p(1);
        p(2) = Data.Recordlength;
        p(1) = 1;
%         p(1)=p(1)-20;
%         p(2)=p(2)+20;
        Data.UsedRecordlength(n) = p(2)-p(1)+1;
        UC(1:Data.UsedRecordlength(n),n) = y(p(1):p(2),1);
        U(1:Data.UsedRecordlength(n),n)= y(p(1):p(2),2);
        %figure
        %plot( U(1:Data.UsedRecordlength(n),n),'color','blue');
        %pause
        I(1:Data.UsedRecordlength(n),n) =0.01*y(p(1)+0:p(2)+0,3);
        %I(1:Data.UsedRecordlength(n),n) =
I(1:Data.UsedRecordlength(n),n) -
(abs(max(I(1:Data.UsedRecordlength(n),n)))-
abs(min(I(1:Data.UsedRecordlength(n),n))))/2;
```

```
       I(1:Data.UsedRecordlength(n),n) =
I(1:Data.UsedRecordlength(n),n) -
mean(I(1:Data.UsedRecordlength(n),n));
              Data.UsedRecordlength=max(Data.UsedRecordlength);
       clear y;
     end
   end
   if n+ii-1 < length(fn)
     l = floor(Data.UsedRecordlength/2);
     Data.I(1:Data.UsedRecordlength,iii) = mean(I,2);
     %Data.I(1:Data.UsedRecordlength,iii) =
Data.I(1:Data.UsedRecordlength,iii)-(Data.I(20,iii)+Data.I(l,iii));
     Data.U(1:Data.UsedRecordlength,iii) = mean(U,2);
     Data.UC(1:Data.UsedRecordlength,iii) = mean(UC,2);
     Data.dt(iii) = dt;
     Data.t(iii) = t;
     Data.filename{iii} = name;
     Data.numfiles = iii;
   end
end

Data.UsedRecordlength = length(Data.I(:,1));

%%%%%%%%%%%%%%%%%%%%%%%%%%%%%%%%%%%%%%%%%%%%%%%%%%%%%%%%%%%%
%%%%%%%%%%%%%      noise filtering    %%%%%%%%%%%%%%%%
%%%%%%%%%%%%%%%%%%%%%%%%%%%%%%%%%%%%%%%%%%%%%%%%%%%%%%%%%%%%

for n = 1 : Data.numfiles
    Data.f_nyquist(n) = 1/(2*Data.dt(n));
% Nyquist frequency
    Param.f_cut = Data.f_nyquist(n)/15
% Hz
    Wn = Param.f_cut/Data.f_nyquist(n);
    [b,a] = butter(3, Wn, 'low');
% 3rd order Bütterworth low-pass filter to supress high frequencies
    Data.I(:,n) = filtfilt(b,a,Data.I(:,n));

    Param.f_cut = Data.f_nyquist(n)/15
% Hz
```

```
    Wn = Param.f_cut/Data.f_nyquist(n);
    [b,a] = butter(3, Wn, 'low');
    Data.U(:,n) = filtfilt(b,a,Data.U(:,n));

end

%%%%%%%%%%%%%%%%%%%%%%%%%%%%%%%%%%%%%%%%%%%%%%%%%%%%%%%%%%%%%%%%%%%%%%%
%%%%%%%%%%%  Curve fitting of probed voltage %%%%%%%%%%%%%
%%%%%%%%%%%%%%%%%%%%%%%%%%%%%%%%%%%%%%%%%%%%%%%%%%%%%%%%%%%%%%%%%%%%%%%
fh_U = @(x,p) p(1)*sin(p(2)*x+p(3));
% fitting function
errfh = @(p,x,y) sum((y(:)-fh_U(x(:),p)).^2);
% Error function

for n = 1 : Data.numfiles
  p0_U = [max(Data.U(1:Data.UsedRecordlength,n)) 2*pi/100 -2.2*pi/100];
% Initial guess for constants
  P_U =
fminsearch(errfh,p0_U,[],(1:Data.UsedRecordlength)*Data.dt(n),Data.U(1:
Data.UsedRecordlength,n));                          % Search for solution
  Data.U(1:Data.UsedRecordlength,n) =
fh_U((1:Data.UsedRecordlength)*Data.dt(n),P_U);
% Replace with fitted data
end


%%%%%%%%%%%%%%%%%%%%%%%%%%%%%%%%%%%%%%%%%%%%%%%%%%%%%%%%%%%%%%%%%%%%%%%
%%%%%%%%%%%%%  find capacitive current  %%%%%%%%%%%%%%%%
%%%%%%%%%%%%%%%%%%%%%%%%%%%%%%%%%%%%%%%%%%%%%%%%%%%%%%%%%%%%%%%%%%%%%%%

corr = (0);
I_C = (0);
for n = 1 : Data.numfiles
    for m = 4 : 2: Data.UsedRecordlength
        if sign(Data.U(m,n))== -1
           if sign(Data.U(m-2,n))==1
              p = m;
           end
       end
```

```
    end
    corr =
Data.I(p,n)/(Param.epsR*Param.eps0*Param.A/Param.d*(Data.U(p,n)-
Data.U(p-1,n))/(Data.dt(n)));              %capacitance correction
factor
    for nn = 2 : Data.UsedRecordlength
         I_C(nn) =
corr*Param.epsR*Param.eps0*Param.A/Param.d*(Data.U(nn,n)-Data.U(nn-
1,n))/(Data.dt(n));
    end
    Data.I_C(1:Data.UsedRecordlength,n) = I_C;
end


%%%%%%%%%%%%%%%%%%%%%%%%%%%%%%%%%%%%%%%%%%%%%%%%%%%%%%%%%%%%%%%%
%%%%%%%%%%%%%     calculate resistivity  %%%%%%%%%%%%%%
%%%%%%%%%%%%%%%%%%%%%%%%%%%%%%%%%%%%%%%%%%%%%%%%%%%%%%%%%%%%%%%%

Data.I_R = zeros(size(Data.I_C));
Data.R = zeros(size(Data.I_C));

for n = 1 : Data.numfiles
    Data.I_R(:,n) = Data.I(:,n)-Data.I_C(:,n);
    Data.R(:,n) = abs(Data.U(:,n)./Data.I_R(:,n));
end


%%%%%%%%%%%%%%%%%%%%%%%%%%%%%%%%%%%%%%%%%%%%%%%%%%%%%%%%%%%%%%%%
%%%%%%%%%%%%%     figure defenition   %%%%%%%%%%%%%%%%
%%%%%%%%%%%%%%%%%%%%%%%%%%%%%%%%%%%%%%%%%%%%%%%%%%%%%%%%%%%%%%%%

f1 = figure(1);
set(f1,'Name','Time
dependence','NumberTitle','off','Position',maxWindow);
ax(1) = subplot(3,1,1); grid on; hold on; xlabel('time (s)');
ylabel('I(t)(A)');
ax(2) = subplot(3,1,2); grid on; hold on; xlabel('time (s)');
ylabel('U(t)(kV)');
```

```
ax(3) = subplot(3,1,3); semilogy(-1,1); grid on; hold on; xlabel('time
(s)');
ylabel('R(t)(ohm)');

f2 = figure(2);
set(f2,'Name','Field
dependence','NumberTitle','off','Position',maxWindow);
ax(4) = subplot(1,1,1);  semilogy(-1,1); grid on; hold on; xlabel('E
(kV/mm)'); ylabel('R(ohm)');



for n = 1 : Data.numfiles

  h = plot(ax(1),(1:Data.UsedRecordlength)*Data.dt(n),Data.I(:,n),'-
','color','blue','LineWidth',1);
  ylim(ax(1),[min(min(Data.I)) max(max(Data.I))]);
set(h,'DisplayName',num2str(Data.t(n)));

  h = plot(ax(1),(1:Data.UsedRecordlength)*Data.dt(n),Data.I_R(:,n),'-
','color','red','LineWidth',1);
  set(h,'DisplayName',num2str(Data.t(n)));

  h =
plot(ax(2),(1:Data.UsedRecordlength)*Data.dt(n),Data.U(:,n)/1000,'-
','color','blue','LineWidth',1);
  ylim(ax(2),[min(min(Data.U/1000)) max(max(Data.U/1000))]);
set(h,'DisplayName',num2str(Data.t(n)));

  h =
semilogy(ax(3),(1:Data.UsedRecordlength)*Data.dt(n),Data.R(:,n),'.','co
lor','red','LineWidth',1);
  ylim(ax(3),[min(min(Data.R)) max(max(Data.R))]);
set(h,'DisplayName',num2str(Data.t(n)));

  h =
semilogy(ax(4),(Data.U(:,n)/1000)/(Param.d*1000),Data.R(:,n),'.','color
','red','LineWidth',1);
```

```
  ylim(ax(4),[min(min(Data.R)) max(max(Data.R))]);
set(h,'DisplayName',num2str(Data.t(n)));

  axes(ax(1));

end
linkaxes([ax(1) ax(2) ax(3)],'x');
xlim(ax(1),[min(min((1:Data.UsedRecordlength)*Data.dt(1)))
max(max((1:Data.UsedRecordlength)*Data.dt(1)))]);

PLOTBROWSER(f1,'on')
PLOTBROWSER(f2,'on')

SurfT = zeros(size(Data.U));
for n = 1 : Data.numfiles
    SurfT(1:Data.UsedRecordlength,n) =
Data.t(n)*ones(1,Data.UsedRecordlength);
end

% f3 = figure(3);
% set(f3,'Name','Field and time
dependence','NumberTitle','off','Position',maxWindow);
% ax(5)=surf(SurfT,Data.U/Param.d,Data.R,'EdgeColor','none'); alpha(1);
% set(gca,'ZScale','log');
% %set(gca,'XDir','reverse');set(gca,'YDir','reverse');
% camlight left; lighting phong
% ylabel('E (kV/mm)'); zlabel('R(ohm)'); xlabel('time');
% ViewT = [-70.5 48.0];
% view(ViewT);
% box on;
% colorbar('location','NorthOutside');

%%%%%%%%%%%%%%%%%%%%%%%%%%%%%%%%%%%%%%%%%%%%%%%%%%%%%%%%%%%%%%%%
%%%%%%%%%%%%%        save data           %%%%%%%%%%%%%
%%%%%%%%%%%%%%%%%%%%%%%%%%%%%%%%%%%%%%%%%%%%%%%%%%%%%%%%%%%%%%%%

Data.Param = Param;
save c:\data Data
```

```
clear answer nn n fn scrsz Wn b a h pks o p mph I U dt t UC iii name
I_C l m mm n P_U p0_U fh_U errfh
```

Appendix 5: Matlab Script for Plotting the Time dependency

```
scrsz=get(0,'ScreenSize');
% screen size
maxWindow=[1 31 scrsz(3) scrsz(4)-104];

E = (0);
E(1) = -10;  %kV/mm, could be changed to users choice
E(2) = +10;
EE = (0);

Rvector = (0);
xnum = (0);
s1 = 2;
s2 = Data.numfiles;
for m = 1 : length(E)
  for n = s1 : s2
    Evector = (Data.U(:,n)/1000)/(Param.d*1000);
     %figure
     %semilogy(Evector,Data.R(:,n));
     %pause
    l3 = length(Evector);
    for o = 1 : l3
      if floor(Evector(o)*20) == floor(E(m)*20)
          xnum(n) = o;
      end
    end
   EE(n,m) = Evector(xnum(n));
    %Evector(xnum(n))
   Rvector(n,m) = Data.R(xnum(n),n);
  end
end

fB1 = figure;
```

```
set(fB1,'Name','Time-evolution of space charge in selected
regions','NumberTitle','off','Position',maxWindow);


for m = 1 : length(E)
    p1 = plot(Data.t(s1:s2)/60,Rvector(s1:s2,m),'.-','color','red');
grid on; hold on;
end
legend(strcat('Field (kV/mm): ',num2str(E(:))));
 xlabel('time (min)'); ylabel('R(t)(ohm)');
```

Appendix 6: Comsol script

```
flclear fem
close all

%%%%%%%%%%%%%%%%%%%%%%%%%%%%%%%%%%%%%%%%%%%%%%%%%%%%%%%%%%%%%%%%%%%%%%%
%%%
%%%%                        Constants & Memory Allocation
%%%%
%%%%%%%%%%%%%%%%%%%%%%%%%%%%%%%%%%%%%%%%%%%%%%%%%%%%%%%%%%%%%%%%%%%%%%%
%%%

GapDist = 2e-3;                     % Gap distance (m)
PlaneDiam = 3.9*10^-2;              % Diameter of plane electrode
V0 = 20000;                         % Voltage amplitude (V)
fAC = 0.1;                          % AC voltage frequencyuency (Hz)
tstop = 1/fAC*0.5;                  % stop time (s)
eps0 = 8.85e-12;                    % vacuum permittivity

gf=rect2(PlaneDiam/2-5e-
3,GapDist,'base','corner','pos',[0,GapDist],'rot','0');

clear draw s
draw.s.objs={gf};
draw.s.name={'CO2'};
draw.s.tags={'gf'};

fem.draw=draw;
```

```
fem.geom=geomcsg(fem);

% % figure
% % geomplot(fem,'pointmode','off','edgecolor','b');
%
% Initialize mesh
fem.mesh=meshinit(fem, ...
                  'hauto',5);

% Refine mesh
fem.mesh=meshrefine(fem, ...
                    'mcase',0, ...
                    'rmethod','regular');

% Refine mesh
fem.mesh=meshrefine(fem, ...
                    'mcase',0, ...
                    'rmethod','regular');

% % Refine mesh
% fem.mesh=meshrefine(fem, ...
%                     'mcase',0, ...
%                     'rmethod','regular');

clear units;
units.basesystem = 'SI';
fem.units = units;


%%%%%%%%%%%%%%%%%%%%%%%%%%%%%%%%%%%%%%%%%%%%%%%%%%%%%%%%%%%%%%%%%%%%%%%%%%%%%%%
%%%
%%%%%%%%%%%%        Determining Application Modes
%%%%%%%%%%%%%%%
%%%%%%%%%%%%%%%%%%%%%%%%%%%%%%%%%%%%%%%%%%%%%%%%%%%%%%%%%%%%%%%%%%%%%%%%%%%%%%%
%%%

% Ionic mobility values from:
% A. Denat, J. P. Gosse, and B. Gosse,
```

```
% "Electrical conduction of purified cyclohexane in a divergent
electric field,"
% IEEE Transactions on Electrical Insulation, vol. 23, pp. 545-54, 1988

% Constants
fem.const = {'mu_ion_pos','3.0e-10[m^2/(V*s)]', ...
  'mu_ion_neg','3.0e-10[m^2/(V*s)]', ...
  'T','290[K]', ...
  'k_boltz','1.38e-23[J/K]', ...
  'q_e','1.6e-19[C]', ...
  'sigma','8e-12[S/m]',...
  'N_A' ,'6.022e23',...
  'V_P', V0,...
  'frequency',fAC,...
  't_stop',tstop};

% Application mode 1
clear appl
appl.mode.class = 'Electrostatics';
appl.mode.type = 'axi';
appl.module = 'ACDC';
appl.assignsuffix = '_es';
clear pnt
pnt.V0 = {0,'V_P*v_func(t)'};
pnt.type = 'V';
pnt.ind = [1,2,1,2];
appl.pnt = pnt;
clear bnd
bnd.V0 = {0,0,'V_P*v_func(t)'};
bnd.type = {'V0','ax','V'};
bnd.ind = [2,1,3,2];
appl.bnd = bnd;
clear equ
equ.epsilonr = 2.02;
equ.rho = '(c-c2)*q_e';
equ.ind = [1];
appl.equ = equ;
fem.appl{1} = appl;
```

```
% Application mode 2
clear appl
appl.mode.class = 'FlConvDiff';
appl.mode.type = 'axi';
appl.assignsuffix = '_cd';
clear prop
prop.equform='cons';
clear weakconstr
weakconstr.value = 'off';
weakconstr.dim = {'lm2'};
prop.weakconstr = weakconstr;
appl.prop = prop;
clear bnd
bnd.c0 = {0,0,'3*c_n0',0};
bnd.type = {'ax','Nc','C','N0'};
bnd.ind = [1,2,3,4];
%bnd.ind = [1,4,4,4];
appl.bnd = bnd;
clear equ
equ.D = 'mu_ion_pos*k_boltz*T/q_e';
equ.init = 'c_n0';
equ.v = 'mu_ion_pos*Ez_es';
equ.u = 'mu_ion_pos*Er_es';
equ.sdon = 1;
equ.sdtype = 'ad';
equ.R = 'c3*k_d0*F_E-c*c2*KR';
equ.ind = [1];
appl.equ = equ;
fem.appl{2} = appl;

% Application mode 3
clear appl
appl.mode.class = 'FlConvDiff';
appl.mode.type = 'axi';
appl.dim = {'c2'};
appl.name = 'cd2';
appl.assignsuffix = '_cd2';
clear prop
prop.equform='cons';
```

```
clear weakconstr
weakconstr.value = 'off';
weakconstr.dim = {'lm3'};
prop.weakconstr = weakconstr;
appl.prop = prop;
clear bnd
bnd.c0 = {0,'3*c_n0',0,0};
bnd.type = {'ax','C','N0','Nc'};
bnd.ind = [1,2,4,3];
%bnd.ind = [1,4,4,4];
appl.bnd = bnd;
clear equ
equ.D = 'mu_ion_neg*k_boltz*T/q_e';
equ.init = 'c_n0';
equ.v = '-mu_ion_neg*Ez_es';
equ.u = '-mu_ion_neg*Er_es';
equ.sdon = 1;
equ.sdtype = 'ad';
equ.R = 'c3*k_d0*F_E-c*c2*KR';
equ.ind = [1];
appl.equ = equ;
fem.appl{3} = appl;

% Application mode 4
clear appl
appl.mode.class = 'FlConvDiff';
appl.mode.type = 'axi';
appl.dim = {'c3'};
appl.name = 'cd3';
appl.assignsuffix = '_cd3';
clear prop
prop.equform='cons';
clear weakconstr
weakconstr.value = 'off';
weakconstr.dim = {'lm3'};
prop.weakconstr = weakconstr;
appl.prop = prop;
clear bnd
bnd.c0 = {0,'c_N0',0,0};
```

```
bnd.type = {'ax','C','N0','Nc'};
bnd.ind = [1,4,4,4];
appl.bnd = bnd;
clear equ
equ.D = '0';
equ.init = 'c_N0';
equ.v = '0';
equ.u = '0';
equ.sdon = 1;
equ.sdtype = 'ad';
equ.R = '-c3*k_d0*F_E+c*c2*KR';
equ.ind = [1];
appl.equ = equ;
fem.appl{4} = appl;


fem.sdim = {'r','z'};
fem.frame = {'ref'};
fem.border = 1;
fem.outform = 'general';
clear units;
units.basesystem = 'SI';
fem.units = units;

% Global expressions
fem.globalexpr = {'KR','q_e*(mu_ion_pos+mu_ion_neg)/epsilon_es', ...
  'cKD','(c_n0)^2*KR*max(F_E,1)', ...
  'b_func','sqrt(q_e^3*normE_es/(16*pi*epsilon_es*k_boltz^2*T^2))', ...
  'F_E','BESSELI(1,4*b_func)/(2*(b_func+1e-9))', ...
  'c_n0','sigma/(q_e*(mu_ion_neg+mu_ion_pos))', ...
  'c_N0','c_n0^2*KR/k_d0', ...
  'K_A', '2.3e20/N_A', ...
  'k_d0','KR/K_A'};

%NB: USE BESSELI and not besseli

% Functions
clear fcns
fcns{1}.type='inline';
```

```
fcns{1}.name='v_func(t)';
fcns{1}.expr='sin(t*0.1*2*pi)';
fcns{1}.dexpr={'cos(t*0.1*2*pi)'};
fem.functions = fcns;


% clear fcns
% fcns{1}.type='inline';
% fcns{1}.name='v_func(t)';
% fcns{1}.expr='flc1hs(t-1e-7,20e-9)';
% fcns{1}.dexpr={'diff(flc1hs(t-1e-7,20e-9))'};
% fem.functions = fcns;


% Descriptions
clear descr
descr.const= {'T','Temperature','q_e','Electron
charge','sigma','Conductivity of liquid','mu_ion_neg','negative ion
mobility','mu_ion_pos','positive ion mobility','k_boltz','Boltzman
constant','mu_el','electron mobility'};
descr.globalexpr= {'KR','Langevin recombination
constant','c_n0','Concentration neutral ion pairs'};
fem.descr = descr;

% ODE Settings
clear ode
clear units;
units.basesystem = 'SI';
ode.units = units;
fem.ode=ode;
% Multiphysics
fem=multiphysics(fem);

% Extend mesh
fem.xmesh=meshextend(fem);

% Solve problem
fem.sol=femtime(fem, ...
               'solcomp',{'V','c','c2','c3'}, ...
```

```
                'outcomp',{'V','c','c2','c3'}, ...
                'tlist',[0:0.01:5], ...
                'tout','tlist');


% Extend mesh
%fem.xmesh=meshextend(fem);

%  fem.sol=femtime(fem, ...
%                  'solcomp',{'V','c','c2','c3'}, ...
%                  'outcomp',{'V','c','c2','c3'}, ...
%                  'tlist',[5:100:10000], ...
%                  'tout','tlist');
%
%%%%%%%%%%%%%%%%%%%%%%%%%%%%%%%%%%%%%%%%%%%%%%%%%%%%%%%%%%%%%%%%%%%%%%%%%%%%%%%
%%
%%%%                        Plot Results
%%%%
%%%%%%%%%%%%%%%%%%%%%%%%%%%%%%%%%%%%%%%%%%%%%%%%%%%%%%%%%%%%%%%%%%%%%%%%%%%%%%%
%%


% Plot solution
% figure; postplot(fem, ...
%          'tridata',{'c','cont','internal','unit','1/m^3'}, ...
%          'trimap','jet(1024)', ...
%          'solnum','end', ...
%          'title','Surface: Concentration, c, norm [1/m^3]');
%
% figure; postplot(fem, ...
%          'tridata',{'normE_es','cont','internal','unit','V/m'}, ...
%          'trimap','jet(1024)', ...
%          'solnum','end', ...
%          'title','Surface: Field norm,norm [V/m]');
%
% figure; postplot(fem, ...
%          'tridata',{'V','cont','internal','unit','V'}, ...
%          'trimap','jet(1024)', ...
%          'solnum','end', ...
```

```
%          'title','Surface: Potential[V]');
%

% Plot in cross-section or along domain
figure; postcrossplot(fem,1,[1], ...
              'lindata','c', ...
              'linxdata','z', ...
              'linlegend','on', ...
              'npoints',2000, ...
              'title','Concentration, c3 [1/m^3]', ...
              'axislabel',{'z','Concentration',' c [1/m^3]'});

% % Plot in cross-section or along domain
% figure; postcrossplot(fem,1,[1], ...
%               'lindata','c2', ...
%               'linxdata','z', ...
%               'linlegend','on', ...
%               'npoints',2000, ...
%               'title','Concentration, c2 [mol/m^3]', ...
%               'axislabel',{'z','Concentration',' c2 [1/m^3]'});
%


%%%%%%%%%%%%%%%%%%%%%%%%%%%%%%%%%%%%%%%%%%%%%%%%%%%%%%%%%%%%%%%%%%%%%%%%%%%%%%%
%%
%%%%                        Post Analysis
%%%%
%%%%%%%%%%%%%%%%%%%%%%%%%%%%%%%%%%%%%%%%%%%%%%%%%%%%%%%%%%%%%%%%%%%%%%%%%%%%%%%
%%

% Get the time vector
timet=fem.sol.tlist;
l = length(timet);

% Displacement current through a chosen plane in the gap
Qimg_plane=postint(fem,'-2*pi*r*(Dz_es)','unit','C','dl',[2], ...
            'edim',1,'solnum',1:1:length(fem.sol.tlist));
I_disp = [0 diff(Qimg_plane)./diff(timet)];
```

```
% Conduction current through a chosen plane in the gap
I_cond_plane =postint(fem,'2*pi*r*(ntflux_c_cd-ntflux_c2_cd2)*q_e', ...
           'unit','A', ...
           'recover','off', ...
           'dl',[2], ...
           'edim',1, ...
           'solnum',1:1:length(fem.sol.tlist));

% Total current (trough any chosen plane in the gap)
I_tot = I_disp + I_cond_plane;

% Displacement current from Laplacian field
U = postint(fem,'V','unit','C','dl',[3], ...
            'edim',1,'solnum',1:1:length(fem.sol.tlist));
U = U./postint(fem,'1','unit','C','dl',[3], ...
            'edim',1,'solnum',1:1:length(fem.sol.tlist));
I_disp_Lap = eps0*pi*(PlaneDiam/2)^2*1/GapDist*[0
diff(U)./diff(timet)];

% Conduction current (non-stationary) at ground electrode
I_cond = I_tot - I_disp_Lap;

R = abs(U./I_cond);

f1 = figure(1);
%set(f1,'Name','Time
dependence','NumberTitle','off','Position',maxWindow);
ax(1) = subplot(3,1,1); grid on; hold on; xlabel('time (s)');
ylabel('I(t)(A)');
plot(timet,I_tot,'color','blue'); hold on;
plot(timet,I_cond,'color','red');
ax(2) = subplot(3,1,2); grid on; hold on; xlabel('time (s)');
ylabel('U(t)(kV)');
plot(timet,U*1e-3,'color','blue');
ax(3) = subplot(3,1,3); semilogy(-1,1); grid on; hold on; xlabel('time
(s)'); ylabel('R(t)(ohm)');
plot(timet,R,'color','blue');
xlim([min(timet) max(timet)]);
```

```
save C:\documents\COMSOL\NewDataC.mat fem;
save C:\documents\COMSOL\NewData.mat fem '-mat';
```

Appendix 7: Results from comsol simulation for 10kV/mm 0.01 Hz electric field

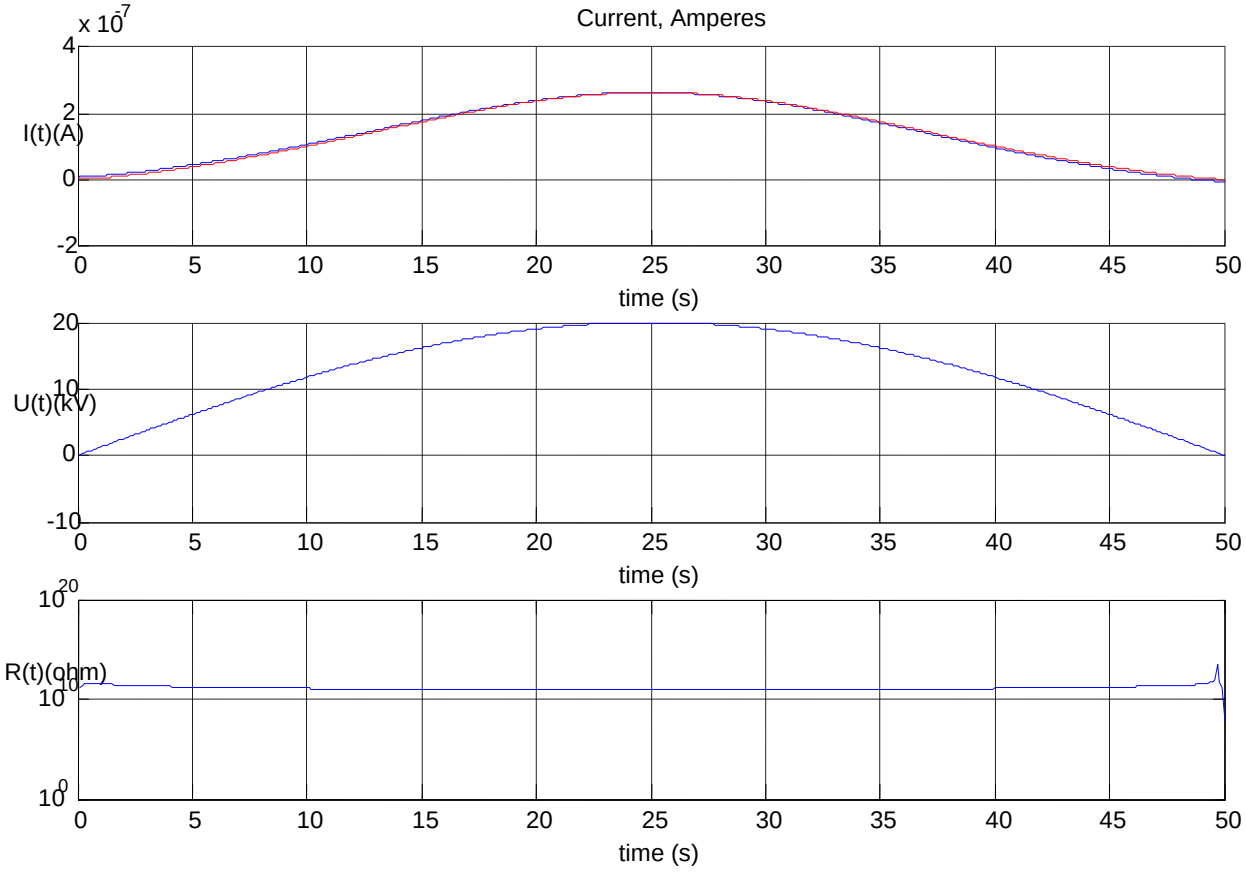

Appendix 8: Comsol Results for 0.1 Hz 10 kV/mm input electric field